https://doi.org/10.5194/egusphere-2025-2559
Preprint. Discussion started: 1 July 2025

A process-evaluation of the impact of precipitation on aerosol particle number size distributions in three Earth System Models

Sara M. Blichner[1,2], Theodore Khadir[1,2], Sini Talvinen[1,2], Paulo Artaxo[3], Liine Heikkinen[1,2], Harri Kokkola[4,5], Radovan Krejci[1,2], Muhammed Irfan[4], Twan van Noije[6], Tuukka Petäjä[7], Christopher Pöhlker[8], Øyvind Seland[9], Carl Svenhag[10,11], Antti Vartiainen[4,12], and Ilona Riipinen[1,2]

[1]Department of Environmental Science, Stockholm University, Stockholm, 10691, Sweden
[2]Bolin Centre for Climate research, Stockholm University, Stockholm, 10691, Sweden
[3]Instituto de Física, Universidade de São Paulo, São Paulo, Brazil
[4]Department of Technical Physics, University of Eastern Finland, Kuopio, 70211, Finland
[5]Finnish Meteorological Institute, Kuopio FI-70211, Finland.
[6]Royal Netherlands Meteorological Institute, De Bilt, Netherlands
[7]University of Helsinki, Institute for Atmospheric and Earth System Research (INAR), Helsinki, Finland.
[8]Multiphase Chemistry Department, Max Planck Institute for Chemistry, 55128 Mainz, Germany
[9]Norwegian Meteorological Institute, Oslo, Norway
[10]Department of Physics, Lund University, Lund, Sweden
[11]Now at: Department of Environmental Science, Aarhus University, Roskilde, Denmark
[12]Advanced Computing Facility, CSC – IT Center for Science Ltd, Espoo, 02150, Finland

Correspondence: Sara M. Blichner (sara.blichner@aces.su.se)

Abstract.

Accurately modeling the cloud condensation nuclei (CCN) budget is a key factor in reducing uncertainty in aerosol–cloud interactions in Earth system models. et deposition – the removal of particles by precipitation – is a major CCN sink, but rainfall can also trigger a replenishment phase via the formation and growth of new particles, partially offsetting losses. In this study, we evaluate how three general circulation models represent the size- and time-resolved effects of precipitation on the particle number size distribution (PNSD) and the CCN budget. The evaluation is based on correlations between the PNSD and the precipitation rates along back trajectories from three long-term measurement stations. To better isolate the role of precipitation from confounding factors, we also apply a Machine Learning approach (XGBoost), training a separate regression model for each site and data source using a minimal set of physically relevant predictors. Our results show that at the two high-latitude stations, the models underestimate CCN replenishment following precipitation, with too weak new particle formation and growth. At ATTO, in contrast, two of the models overestimate this effect, simulating an immediate CCN source after rainfall. Observations also suggest that CCN removal is weaker during colder conditions, a pattern that models struggle to capture – either overestimating or underestimating the precipitation effect, depending on the model. The XGBoost analysis confirms the key findings of the correlation analysis while helping to correct for likely confounding influences, showing promise for disentangling spurious correlations and controlling for unrelated factors in model evaluation.

https://doi.org/10.5194/egusphere-2025-2559
Preprint. Discussion started: 1 July 2025

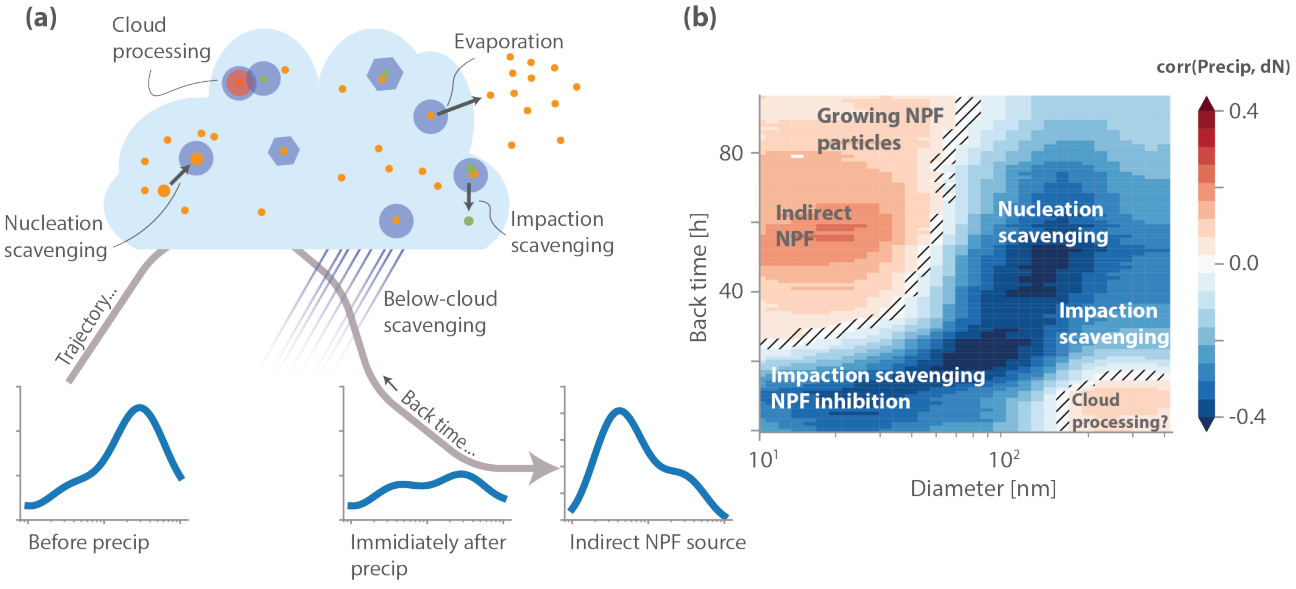

Figure 1. Illustratration of precipitation impact on particle number size distribution (PNSD). Panel a shows an illustration of the main processes and their impact on an idealized size distribution: An imagined accumulation mode dominated size distribution before the rain, is then influenced by in-cloud nucleation and impaction scavenging in addition to below cloud scavenging, reducing in particular the accumulation and coarse mode particle concentration. This primes the atmosphere for new particle formation (NPF) if precursors become available due to the low condensation/coagulation sink (indirect NPF from rain), thus creating a growing NPF and Aitken mode. Panel b shows how these processes would be expected to show up in the correlation analysis where precipitation rates along the back trajectories at different point back in time ("back time") are correlated with the observed size distribution at the station. Impaction scavenging (both in and below cloud) shows up strongly for the smallest and largest particles, nucleation scavenging is strongest for particles larger than the activation diameter (usually between 50–200 nm), indirect NPF shows up for less recent precipitation (40+ hours back in time) and with a potentially growing mode as back time increases. Finally an observed positive correlation between recent precipitation and accumulation mode particles (bottom right corner) has been hypothesised to be related to cloud processing. The correlation plot in (b) is from observations in Hyytiälä, during spring (MAM). The cloud illustration in (a) is inspired by Hoose et al. (2008a).

1 Introduction

Aerosol particles in the atmosphere are vital players in both climate (Forster et al., 2021) and human health (Lelieveld et al., 2019; Schraufnagel, 2020). The climate impact is dominated by aerosol-cloud interactions, mainly through particles that act as cloud condensation nuclei (CCN) (Forster et al., 2021) and thus cooling the surface by making clouds more reflective (Twomey, 1959, 1974) and potentially longer-lived (Albrecht, 1989). Capturing the main features of the CCN budget is therefore a major concern for any climate or weather model.

https://doi.org/10.5194/egusphere-2025-2559
Preprint. Discussion started: 1 July 2025

Although a fair amount of attention has been paid to evaluating model performance of the CCN source term, e.g., studying new particle formation (NPF; see e.g. Svenhag et al., 2024; Olenius and Riipinen, 2017; Roldin et al., 2019) and emissions (see e.g. Moseid et al., 2020; Blichner et al., 2024), less attention has been paid to directly evaluating the sink term. In parts, this is likely because source processes are often easier to observe with "nucleation bananas" (e.g. Kulmala et al., 2004) or emission sources that are obvious in the measurements. Model evaluations focused on sinks, e.g., via precipitation (wet deposition), on the other hand, usually report effects on the average concentration, the vertical profiles, and so on (e.g. Holopainen et al., 2020; Kipling et al., 2016).

The deposition of particles is generally separated into wet deposition and dry deposition, where wet deposition refers to removal via clouds and precipitation, while dry deposition involves the particles depositing onto the surface without the aid of precipitation. For most aerosol species and sizes, wet deposition dominates the removal processes (Textor et al., 2006; Bourgeois and Bey, 2011; Kipling et al., 2016; Emerson et al., 2018). Wet deposition is divided further into *in-cloud* and *below-cloud* scavenging. In-cloud scavenging refers to the particles taken up into cloud droplets or ice crystals – either via nucleation (acting as CCN or INP, nucleation scavenging) or via coagulation with cloud droplets or ice crystals (impaction scavenging) – and these are then lost from the atmosphere if the cloud hydrometeors end up forming precipitation which reaches the surface. Below-cloud scavenging refers to the process in which particles are scavenged by falling rain droplets and snow (below-cloud impaction scavenging).

The size dependence of the different loss processes is illustrated in Fig. 1. Nucleation scavenging is efficient for CCN sized particles in general (depending on hygroscopicity and supersaturation conditions), while in-cloud and below-cloud impaction scavenging is more efficient for particles larger or smaller than the accumulation mode: larger particles due to their greater inertia, which makes them more likely to collide with rain drops, and smaller particles due to the effect of Brownian motion, which also increases their collision probability (Greenfield, 1957; Seinfeld and Pandis, 2016).

Models vary in complexity in their treatment of wet deposition. The simplest approach is to prescribe aerosol scavenging fractions for in-cloud and below-cloud scavenging separately, usually divided into aerosol type (composition and size) (e.g. Stier et al., 2005; Iversen and Seland, 2002) as well as cloud type (convective versus stratiform) and even temperature (to represent cloud phase) (see e.g. discussion in Hoose et al., 2008b). The next step of complexity used for in-cloud scavenging is to explicitly model interstitial versus cloud-borne particles based on, e.g., activation rates and coagulation and then compute wet deposition based on the precipitation production rate (see e.g. Croft et al., 2010; Hoose et al., 2008b). This can be done both diagnostically, where the cloud-born aerosol is diagnosed in each time step based on various factors (e.g. Hoose et al., 2008a; van Noije et al., 2021), or prognostically, where the cloud-born aerosol is additionally passed between time steps (e.g. Hoose et al., 2008a).

As mentioned above, in-cloud scavenging can be separated into nucleation and impaction scavenging. If the model uses fixed prescribed scavenging ratios, they will usually implicitly combine the two. However, for more advanced treatments, nucleation scavenging may be connected to the activation rate, and the collection of aerosols by cloud droplets and ice crystals requires a separate treatment. This can then, for example, be done by using a collection kernel for each aerosol type (mode or otherwise) or other parameterizations or look-up table approaches (Hoose et al., 2008a; Croft et al., 2010; Holopainen et al.,

https://doi.org/10.5194/egusphere-2025-2559
Preprint. Discussion started: 1 July 2025

2020). Separate treatments are usually applied for convective clouds and stratiform clouds (Croft et al., 2010; Browse et al., 2012), especially because GCMs tend not to represent aerosol effects on cloud microphysics for convective clouds. This means that convective cloud scavenging is usually much more simplified.

Additionally, choices usually have to be made with respect to how to treat ice clouds versus liquid clouds and precipitation (e.g. Seland et al., 2008; Stier et al., 2005; Croft et al., 2010; Ryu and Min, 2022; Holopainen et al., 2020). In general, precipitation formed via ice formation is expected to scavenge less aerosols than liquid precipitation formation. This is because while liquid precipitation is formed via collision coalescence, thus scavenging CCN from all collected cloud droplets, precipitation initiated via ice can be formed via deposition growth of a single ice crystal, sometimes at the expense of surrounding supercooled cloud droplets which will then rerelease the CCN particles (the Wegener-Bergeron-Findeisen process Bergeron, 1935; Findeisen, 1938; Wegener, 1911) (see e.g. Browse et al., 2012). However, riming is likely to efficiently scavenge CCN as a result of the collection of supercooled droplets. To summarize: Warm precipitation effectively scavenges CCN, precipitation from fully glaciated clouds is likely less efficient, while mixed clouds are a challenge.

Falling rain evaporation is often ignored in GCMs in terms of its impact on aerosol transport (all scavenged aerosols are often assumed to reach the surface) (e.g. Ryu and Min, 2022; Kipling et al., 2016), but it has been explored, for example, in the EC-Earth model (de Bruine et al., 2018) and partially in HadGEM3–UKCA (Kipling et al., 2016). The goal of de Bruine et al. (2018) was to investigate the effects of the rerelease of aerosols from precipitation evaporation. They showed that including this rerelease process leads to higher aerosol concentrations in the lower atmosphere, but it was highly region- and season-dependent. In general, the effect will depend on assumptions concerning the cloud processing of the aerosols, i.e. what happens to composition and size during the cloud and precipitation formation. Kipling et al. (2016) investigated various factors and their effect on the vertical particle profiles in HadGEM3–UKCA including the effect of reevaporation and did not find that reevaporation had a large impact compared to other factors.

For in-cloud scavenging, research suggests that nucleation scavenging dominates over impaction scavenging for accumulation mode particles (Ohata et al., 2016; Moteki et al., 2012; Taylor et al., 2014; Flossmann et al., 1985; Flossmann and Wobrock, 2010). Croft et al. (2010) compared different wet deposition representations for in-cloud scavenging in ECHAM5-HAM and found that with their diagnostic representation of cloud-borne aerosol, aerosol mass was primarily scavenged by nucleation, while number was primarily scavenged by impaction (>90 %). They also found large differences in predicted global mean aerosol mass burdens (20-30%) depending on the in-cloud deposition scheme, and even larger changes in the accumulation mode number concentration (up to 50%). Differences were found to be particularly large in areas with mixed phase and ice clouds. Ryu and Min (2022) suggest that below-cloud scavenging may be underestimated (at least in their version of WRF-Chem) based on empirical evidence from Northern China and India. Their updated model decreases the in-cloud wet scavenging fraction from 88-95% to 34–37% with the associated increase in below-cloud scavenging. Holopainen et al. (2020) compare the ECHAM-SALSA model with fixed prescribed scavenging coefficients with an updated, size-dependent scheme for both nucleation and in-cloud impaction scavenging. They find that the new scheme yields higher concentrations of particles larger than 100 nm and a decrease below, when compared to the fixed scavenging fractions. They explain this with

https://doi.org/10.5194/egusphere-2025-2559
Preprint. Discussion started: 1 July 2025

more efficient impaction scavenging and less efficient nucleation scavenging as compared to the original formulation using prescribed coefficients.

Finally, uptake of particles in cloud droplets will often not result in them raining out, as most cloud droplets evaporate rather than precipitate. Pruppacher et al. (1998) estimate that an aerosol particle may go through about ten cloud cycles (activation and subsequent evaporation) during their lifetime. As cloud water acts as a reactive medium, it also has the potential to shape the properties of aerosol particles. This means that the properties of an aerosol particle that is activated to form a cloud droplet are different once the cloud water evaporates. Sulfate formation in cloud water is currently recognized as an important cloud processing pathway, significantly contributing to the global sulfate aerosol burden and the growth of CCN while also increasing their hygroscopicity (e.g. Ervens, 2015). The scavenging of interstitial particles can also cause similar effects when the particles are taken up by cloud water. In terms of cloud processing, most models only represent aqueous phase sulfate production with varying choices as to how to distribute this sulfate amongst particles (e.g. Lohmann et al., 2001).

While wet deposition is typically viewed as a sink for aerosols, Khadir et al. (2023) demonstrated that precipitation also has important indirect effects on the aerosol lifecycle. Using a lagged, trajectory-based correlation method applied to size-resolved aerosol data, the study showed that rain events act as a reset of the particle number size distribution (PNSD): by removing existing particles through wet scavenging, precipitation reduces the condensation and coagulation sinks, which creates conditions for new particle formation (NPF) and early growth. At the same time, the cloud cover associated with rain suppresses solar radiation and photochemistry, temporarily delaying NPF. The result is a distinct interplay: rain first removes particles, but then creates post-rain conditions that favor the build-up of a new aerosol population – a "replenishment phase" that often occurs hours after rainfall. This framework highlights how precipitation influences both removal and re-formation of particles, offering a process-level interpretation of changes across the aerosol size spectrum.

NPF and subsequent particle growth remain as major uncertainties in climate models. Model estimates of their influence on CCN-relevant particle concentrations (e.g., N_{100}) vary widely and depend strongly on how organic aerosol contributions to growth are represented (see e.g. section V in Stolzenburg et al., 2023). Some models show that NPF increases CCN concentrations (Gordon et al., 2017; Merikanto et al., 2009), while others simulate a decrease: more particles form, but fewer grow large enough (Sullivan et al., 2018; Blichner et al., 2021; Patoulias et al., 2024; Roldin et al., 2019). Observing this growth is difficult at a single station due to air mass variability and boundary layer dynamics (e.g. Hakala et al., 2019), which complicates model evaluation. However, the correlation-based approach developed by Khadir et al. (2023), offers a way to assess these processes systematically. By linking past rainfall to changes in the PNSD, it captures how precipitation resets the aerosol population and sets the stage for post-rain NPF and growth. The results of that study show a growing NPF mode after rainfall at the two high-latitude stations where NPF is frequent, Hyytiälä SMEAR-II (boreal forest) and Zeppelin (arctic) during the relevant seasons. At the tropical ATTO site, however, the picture is different: NPF is not observed in the boundary layer (Zhu et al., 2025), but recent precipitation correlates positively with an increase in smaller particles. These likely originate from higher altitudes, where particle populations are richer in smaller sizes (Curtius et al., 2024; Andreae et al., 2018), and are likely transported into the boundary layer by downdrafts associated with precipitation (Wang et al., 2016). Another hypothesis is that

https://doi.org/10.5194/egusphere-2025-2559
Preprint. Discussion started: 1 July 2025

precipitation injects ozone into the boundary layer, leading to increased concentrations of oxidized biogenic volatile organic compounds, which might enhance conditions for boundary-layer NPF (Machado et al., 2024).

Khadir et al. (2023) further demonstrated the importance of separating aerosol sizes and the timing of precipitation to obtain a good understanding of the process. This is illustrated in Fig. 1b which is an adaptation of a figure from Khadir et al. (2023) and shows the correlation between the PNSD measured at Hyytiälä measurement station (Finland) and the precipitation rate along the back trajectories from the same station. With full resolution in both aerosol size and timing of precipitation, patterns emerge which would be overlooked if we were to for example look at just number, mass or accumulated precipitation.

In this study, we evaluate the time-resolved precipitation impact on the PNSD using the approach developed in Khadir et al. (2023), in three different general circulation models (GCMs) which can be run as Earth System Models (ESMs). We use nudged simulations with high temporal resolution output, combined with trajectories derived with HYSPLIT to extract precipitation rate along the back trajectories in the models. This is then used to compute correlations with PNSD at the three measurement stations representing three different environments: Hyytiälä in the boreal forest, Zeppelin in the Arctic and ATTO station in the Amazon rainforest. To further investigate potential confounding factors influencing particle number size distributions (PNSD), we complement our relatively simple correlation analysis with a more flexible machine learning approach. Specifically, we employ eXtreme Gradient Boosting (XGBoost), a powerful and interpretable tree-based ensemble method known for its performance in capturing complex nonlinear relationships and interactions among predictors. By constructing separate XGBoost regression models for each data source (model outputs and observations), we aim to assess the contribution of precipitation to variations in the particle number concentrations, while also accounting for other relevant variables. We incorporate a minimal, yet representative set of meteorologically and chemically relevant predictors: precipitation rate, air mass trajectory position, time of day, and day of year. This approach allows us to further isolate and quantify the effect of rain on PNSD in a more nuanced way, and to evaluate whether modeled and observed systems respond similarly to key environmental drivers.

2 Methods

2.1 Model descriptions

Table 1 summarizes the treatment of wet deposition in the different models.

2.1.1 ECHAM-SALSA

General description: The global aerosol-climate model ECHAM-SALSA (ECHAM6.3-HAM2.3; Schultz et al., 2018) is widely used to simulate the complex interactions between aerosols, clouds, and the broader climate system. ECHAM-SALSA consists of the general circulation model ECHAM6.3, which captures large-scale atmospheric dynamics by solving equations for divergence, temperature, surface pressure, and vorticity. ECHAM employs a spectral method for calculating the atmospheric circulation and we use the T63 spectral truncation for the horizontal grid, with 47 flexible vertical levels.

https://doi.org/10.5194/egusphere-2025-2559
Preprint. Discussion started: 1 July 2025

	NorESM	EC-Earth	ECHAM-SALSA
Stratiform clouds (strat. cl.): Nucleation scavenging	Cloud-borne aerosol calculated based on droplet activation rate (Abdul-Razzak and Ghan, 2000) for liquid clouds and ice nucleation for ice. Scavenging calculated based on total cloud-born aerosol.	In-cloud scavenging is described using prescribed mode-dependent scavenging fractions (Bourgeois and Bey, 2011). See Table 2 in van Noije et al. (2021)	Nucleation scavenging is based on activated fraction. For liquid it is based on Abdul-Razzak and Ghan (2002), for ice it is based ice crystal number concentration and the relative surface area of each aerosol size class.
Strat. cl.: In-cloud impaction scavenging	Cloud-borne aerosol calculated based coagulation with droplets of assumed size of 10 µm and only considered for Aitken mode and BC in the Accumulation mode. No separate treatment for ice clouds.	Not separate from nucleation scavenging, see above.	Impaction scavenging coefficients are calculated following Croft et al. (2010) and depends on the aerosol particle radius and the droplet radius. Same for ice and liquid, though ice is assumed to be monodisperse (have the same size).
Strat. cl.: Prognostic cloud-borne particles?	Yes.	No.	No.
Stratiform clouds: Phase dependency on in-cloud scavenging	Yes, nucleation scavenging is different for ice and liquid, but impaction scavenging is the same (see above).	Different scavenging fractions for liquid (>0 °C), mixed-phase (-35–0 °C) and ice (<-35 °C) clouds.	Yes, nucleation scavenging is different for ice and liquid nucleation (see above) and impaction scavenging for ice clouds assumes ice crystals are monodisperse.
Below-cloud scavenging	Scavenging coefficients per mode. Following Dana and Hales (1976); Balkanski et al. (1993) as described in Barth et al. (2000).	Scavenging coeffients per mode estimated based on Croft et al. (2009). Differentiates between scavenging coefficients for mass and number and therefore leads to a change in the mean/median particle size of the modes.	Scavenging coeffeficients per bin estimated based on Croft et al. (2009), with each size bin approximated as a log-normal mode. Separate for stratiform and convective clouds and for rain and snow.
Phase dependency for below-cloud scavenging	No.	No	Yes, differentiates collection efficiency of raindrops and snow following Croft et al. (2009).
Redistribution of aerosol due to precipitation evaporation	Yes, for stratiform in-cloud scavenging.	No, not in standard setup.	No.
Aerosol transport in convective up- and downdrafts?	Yes, with a bulk mass-flux scheme following a modified version of Zhang and McFarlane (1995).	Yes, using a modified version of the bulk mass flux scheme of Tiedtke (1989) as applied in IFS cycle 36r4, with a diagnostic convective closure dependent on the convective available potential energy (Bechtold et al., 2014).	Yes, with mass-flux scheme of Tiedtke (1989) with modifications by Nordeng (1994).

Table 1. Comparison of wet deposition and scavenging processes across NorESM, EC-Earth, and ECHAM-SALSA.

https://doi.org/10.5194/egusphere-2025-2559
Preprint. Discussion started: 1 July 2025

ECHAM is coupled with HAM (Hamburg Aerosol Model), which simulates the atmospheric aerosol life cycle, including emissions, formation, growth, and removal (Kokkola et al., 2018; Tegen et al., 2019). The chemical compounds included in HAM are sulfate (SU), organic aerosol (OA), sea salt (SS), black carbon (BC), and mineral dust (DU). HAM includes detailed representations of secondary organic aerosol (SOA) formation, aerosol–radiation interactions, and aerosol–cloud interactions. ECHAM-HAM is further coupled with the Sectional Aerosol module for Large Scale Applications (SALSA; Kokkola et al., 2018). SALSA provides a size-resolved treatment of aerosol microphysics using a sectional approach. The aerosol size spectrum is divided into 10 size bins ranging from 3 nm to 10 µm, with parallel externally mixed size classes for particles larger than 50 nm (Kokkola et al., 2018). SALSA simulates key processes such as nucleation, coagulation, condensation/evaporation, and hydration. Cloud droplet activation is represented using the parameterization by Abdul-Razzak and Ghan (2002), which calculates the fraction of particles activated within each size bin. The module tracks several chemical species, including sulfate, organic carbon, black carbon, sea salt, and mineral dust.

ECHAM-SALSA includes the Volatility Basis Set (VBS) framework to represent SOA formation based on the volatility distribution of organic compounds. By default, ECHAM-SALSA uses a three volatility bin VBS setup for monoterpene oxidation products with C_{sat} values of 0, 1, and 10 μm^{-3} (Mielonen et al., 2018; Irfan et al., 2024).

In the simulations in this study, nudging was applied toward the ERA-Interim reanalysis data from the European Centre for Medium-Range Weather Forecasts (Berrisford et al., 2011). The relaxation times applied for nudging surface pressure, vorticity, and divergence were 24, 6, and 48 hours, respectively.

Wet deposition:

Nucleation scavenging in stratiform clouds: For stratiform clouds ECHAM-SALSA uses size dependent schemes for in-cloud nucleation scavenging detailed in Holopainen et al. (2020). For liquid phase, the in-cloud nucleation scavenging coefficients are calculated using the fraction of activated particles in each size class using the parameterization (Abdul-Razzak and Ghan, 2002). For ice phase, size-dependent scavenging coefficients are calculated based on the surface area of each size class.

In-cloud impaction scavenging in stratiform clouds: The coefficients are based on coagulation rates using wet aerosol particle size and cloud droplet radii and are thus size dependent. Additionally, separate coefficients are calculated for ice crystals, assuming these are monodisperse(see Croft et al., 2010; Holopainen et al., 2020).

Convective cloud scavenging: For convective clouds ECHAM-SALSA uses fixed scavenging coefficients (Bergman et al., 2012). There is no phase dependency on these parameters.

Below cloud scavenging: For below-cloud scavenging in both convective and stratiform clouds, the method of Croft et al. (2009) is used, with each size bin approximated as a log-normal mode. The size-dependent collection efficiency is based on the aerosol and collector drop (raindrops follow the distribution of Marshall and Palmer (1948)) following Croft et al. (2009) and is calculated separately for stratiform and convective clouds, for rain and snow (Croft et al., 2009; Zhang et al., 2012).

Resuspension of aerosols when precipitation evaporates: Resuspension of aerosols when precipitation evaporates is treated so that aerosols from evaporated clouds are released back from the clouds only if the evaporation occurs in the same grid box as precipitation formation. There is no vertical redistribution of aerosol due to precipitation.

https://doi.org/10.5194/egusphere-2025-2559
Preprint. Discussion started: 1 July 2025

Phase dependency: In ice clouds, nucleation scavenging in stratiform clouds involves the formation and growth of ice particles, which can grow to precipitation sizes and be removed. The model accounts for ice nucleation rates and defines the scavenging coefficient values based on the surface are of particles in each size class (see Holopainen et al., 2020). Also for below-cloud scavenging, the model considers the collection efficiency of raindrops and snowflakes differently.

2.1.2 EC-Earth

General description:

In this study, we employ the atmosphere-only AerChem configuration of the Earth system model EC-Earth3.4, which couples a general circulation model (GCM) with an atmospheric chemistry transport model (van Noije et al., 2021, 2014). The GCM component is based on cycle 36r4 of the Integrated Forecasting System (IFS), utilizing a spectral truncation of T255 (approximately 0.7° horizontal resolution) on an N128 reduced Gaussian grid, with 91 vertical levels represented on a hybrid sigma-pressure coordinate system (Döscher et al., 2022). Atmospheric chemistry and aerosol processes are simulated using version 1.2 of the Tracer Model 5 with massively parallel (TM5-MP), which includes the M7 aerosol microphysics module (Vignati et al., 2004; Krol et al., 2005; Williams et al., 2017). TM5-MP operates on a $2^\circ \times 3^\circ$ (latitude $\times$ longitude) horizontal grid and 34 hybrid sigma-pressure levels, which are derived from the same vertical structure used in IFS.

In the simulations in this study, nudging was applied to the IFS model using a relaxation time of 6 hours to ERA-Interim (Berrisford et al., 2011) meteorological fields for divergence, vorticity (horizontal winds), and surface pressure.

Wet deposition:

Precipitation fields for calculating wet deposition in TM5 are received from the IFS model with a coupling time of 6 hours.

In-cloud scavenging: Wet removal of aerosols in EC-Earth is parameterized using prescribed mode-dependent scavenging fractions following Croft et al. (2010) with coefficients from Stier et al. (2005) for convective clouds and Bourgeois and Bey (2011) for stratiform in-cloud scavening (see Table 2 in van Noije et al. (2021)). There is also no distinction between in-cloud activation and impaction scavenging, but rather these are combined in one scavenging fraction. The stratiform in-cloud scavenging is phase dependent, with higher removal for liquid clouds than ice (see Table 2 van Noije et al., 2021).

Below cloud scavenging: Below cloud scavenging by stratiform precipitation applies scavenging coefficient for each mode separately, and for number and mass separately (see Table 3 in van Noije et al. (2021)). These are based on results from Croft et al. (2009) and calculated for a Marshall-Palmer rain droplet size distribution and precipitation rate of $1\,\mathrm{mmh}^{-1}$. This in effect shifts the size distribution, with nucleation and Aitken modes to larger sizes and accumulation and coarse to smaller (van Noije et al., 2021). For convective clouds, below cloud scavenging is included in the fractions described above.

Resuspension of aerosols when precipitation evaporates: Not treated in this version of the model, but investigated in de Bruine et al. (2018).

Phase dependency: There is a phase dependency for stratiform in-cloud scavenging (see again Table 2 in van Noije et al., 2021), with different coefficients for each mode. For below-cloud scavenging there is no phase dependency.

https://doi.org/10.5194/egusphere-2025-2559
Preprint. Discussion started: 1 July 2025

2.1.3 NorESM

General description: The Norwegian Earth System model version 2 (NorESM2 Bentsen et al., 2013; Kirkevåg et al., 2013; Iversen et al., 2013) is based on the Community Earth System Model (CESM Danabasoglu et al., 2020), but features a different ocean model – the Bergen Layered Ocean Model (BLOM) – along with significant modifications to the atmospheric component, including a distinct chemistry and aerosol model (Seland et al., 2020). In this study sea surface temperatures and sea ice data based on the Hadley Centre Sea Ice and Sea Surface Temperature data set (HADISST, Rayner et al., 2003) as described in Hurrell et al. (2008) were read from file, so the ocean component is not in use. The atmospheric component used in NorESM, CAM6-Nor, is heavily based on the Community Atmospheric model version 6 (CAM6, see e.g Bogenschutz et al., 2018) but the aerosol scheme is replaced by OsloAero6 (described below, see also Kirkevåg et al., 2018) and it also include improvements to the local dry and moist energy conservation, angular momentum conservation and in the computation of air-sea fluxes and deep convection. CAM6-Nor uses the same cloud macrophyiscs scheme as CAM6, namely the Cloud Layers Unified by Binomials model (CLUBB; Bogenschutz et al., 2018), as well as the same microphysics in shallow convection and stratiform clouds, which is the two-moment bulk scheme from MG2, Gettelman and Morrison (2015). Finally, the representation of microphysics in deep convective clouds is based on Zhang and McFarlane (1995). Cloud droplet activation is calculated using the Abdul-Razzak scheme (Abdul-Razzak and Ghan, 2000). More details on the treatment of clouds in CAM6 and CAM6-Nor can be found in Bogenschutz et al. (2018).

OsloAero6 is an aerosol and chemistry model that employs a production-tagging approach to track the origin and transformation of aerosols throughout their atmospheric lifetime. A key distinguishing feature of this scheme is its division of aerosol tracers into two categories: "background" tracers and "process" tracers. Background tracers define the initial particle number and size distribution, which follows log-normal modes. In contrast, process tracers modify this distribution and adjust chemical composition based on precomputed look-up tables from the offline AeroTab scheme (Kirkevåg et al., 2018), allowing for deviations from a strict log-normal shape.

In the simulations in this study, nudging was applied using ERA-Interim (Berrisford et al., 2011) data for horizontal winds and surface pressure with a 6-hour relaxation time.

Wet deposition:

Nucleation scavenging in stratiform clouds NorESM keeps track of cloud-borne aerosols (prognostic variable) for stratiform clouds and uses this to calculate the nucleation scavenging. The nucleation scavenging is thus composition and size dependent through the activation scheme following Abdul-Razzak and Ghan (2000). The cloud-borne aerosols are then scavenged based on the precipitation rate.

In-cloud impaction scavenging in stratiform clouds: Additionally, the cloud-borne particles include particles coagulating with cloud droplets, which is calculated assuming a fixed cloud droplet size of 10 μm. The total in-cloud wet deposition then depends on a first-order loss rate calculated from cloud fraction, cloud water, and precipitation production profiles.

Convective clouds scavenging: For convective clouds, both nucleation scavenging and activation scavenging are parameterized by scavenging coefficients. Cloud-born aerosols are not scavenged by convective precipitation, only interstitial aerosols are.

https://doi.org/10.5194/egusphere-2025-2559
Preprint. Discussion started: 1 July 2025

Activation scavenging is controlled by an activation fraction coefficient (set to be 0.8) which controls the fraction of aerosols assumed to activate and a scavenging fraction (sol_factic, set to be 0.4) which is considered a tuning factor. These factors are independent of aerosol size and composition.

Below cloud scavenging: This is parameterized following Dana and Hales (1976); Balkanski et al. (1993) Barth et al. (as described in 2000). It is calculated based on a solubility factor (a tuning factor set to 0.1), multiplied by a scavenging coefficient which varies with mode (see Tab. S1) and the precipitation rate. Cloud-borne aerosols are not subject to below-cloud scavenging.

Resuspension of aerosols when precipitation evaporates: CAM-Oslo treats this, and in the case of evaporating precipitation the aerosol is resuspended proportional to the evaporation rate of precipitation from the layer above and the loss of aerosols from the layer above (if some x percent of the rain evaporates, then x percent of the scavenged aerosol is re-released in the grid box below (Barth et al., 2000).

Phase dependency: Wet deposition is not influenced by precipitation phase, neither for -below, nor for in-cloud scavenging.

2.2 Observations

The observational data is identical to that used in Khadir et al. (2023), and details can be found there. For the station data, we use Scanning or Differential Mobility Particle Sizer (S/DMPS) data from the three stations for the PNSD. The data is originally in hourly resolution, but is reduced to 3-hourly resolution to be comparable to the model output. The non-refractory aerosol composition data for Hyytiälä is from an Aerosol Chemical Speciation Monitor (ACSM) from Heikkinen et al. (2020), while the eBC concentrations are attained from Aethalometer measurements (Luoma et al., 2019) as described in Ranjan et al. (2025).

2.3 Re-analysis data for precipitation

For Zeppelin and Hyytiälä, we use ERA5 reanalysis data ('total_precipitation') in 3 hourly time resolution from C3S (2018), regridded from $0.25 \times 0.25°$ to $1 \times 1°$ resolution in order to be more consistent with the models resolution. As in Khadir et al. (2023), for ATTO we use the TRMM 3B42 V7 satellite product ($0.25° \times 0.25°$, 3-hourly time resolution) (Michot et al., 2018) due to the limitations of re-analysis data in the tropical region in capturing convective precipitation. For simplicity, we refer to the re-analysis and satellite product as 'Observations' below.

2.4 Model data

All models used in this study provided precipitation data at 3-hourly time resolution with full spatial coverage. Aerosol particle size distribution data was also output for the model grid cell covering each station in the same time resolution, together with composition data. All simulations were performed with meteorological nudging to ERA-Interim (Berrisford et al., 2011) reanalysis data (see Sect. 2.1 for details), which ensures that the large-scale dynamics in the models are constrained by observed meteorology.

https://doi.org/10.5194/egusphere-2025-2559
Preprint. Discussion started: 1 July 2025

The composition data from the models used in Fig. 10 include only modes or bins below 1 µm to be comparable to the ACSM data. Note also that for EC-Earth, the sulfate only includes Accumulation mode and Nucleation mode, because the Aitken mode sulfate was unfortunately not output. However, the Accumulation mode dominates the mass signal and should correlate fairly well with the Aitken mode mass, so the error should be minor.

2.5 Trajectory analysis

We use a trajectory-based approach to investigate the relationship between precipitation and aerosol properties. Back trajectories were computed using HYSPLIT with GDAS1 reanalysis data. The precipitation rate from model output, ERA5 reanalysis data (for Zeppelin and Hyytiälä) and TRMM satellite product (for ATTO) were then co-located to the trajectories with nearest-neighbour method. The approach is similar to Talvinen et al. (2025), but instead of calculating the back trajectories with the model output data – which would require internal wind fields – we assume the GDAS1 derived back trajectories have similar large-scale dynamics as ERA-Interim, to which the models are nudged. Although the nudging is not done with GDAS1 directly, previous work (Heslin-Rees et al., 2024; Isokääntä et al., 2022; Talvinen et al., 2025) has indeed shown that back trajectories computed with GDAS1 and ERA-Interim are comparable. This supports the assumption that air mass paths in the nudged model simulations are sufficiently close to those derived from GDAS1 to allow direct comparisons. As a result, model variables can be sampled along the same air mass histories as observations, enabling a consistent and physically meaningful evaluation. Note also that any uncertainty introduced by using trajectory calculated from re-analysis rather than from the native model data is likely comparable to the uncertainty introduced by using re-analysis to analyse the observations – i.e. the "real" trajectory is likely as far or further away from the re-analysis based one as the "real" model trajectory is. All aerosol size distribution data, both from observations and models, are taken from the station (observations) or the grid cell that covers the station (models).

For "observational" precipitation, we apply the same trajectory-based sampling approach using ERA5 reanalysis data for Zeppelin and Hyytiälä, and the TRMM 3B42 V7 satellite product for ATTO. The supplement Figs. S9–S15 shows a comparison between using GDAS precipitation extracted with HYSPLIT versus using the ERA5 data collocated.

To quantify the link between precipitation and particle concentrations, we calculate Spearman's rank correlation coefficients between precipitation intensity at each back-trajectory time step and the particle number concentrations in each size bin. This nonparametric metric captures monotonic relationships, making it suitable for identifying systematic increases or decreases in particle number concentration with varying precipitation intensity, even when the relationship is not linear.

2.6 XGBoost model

Correlating precipitation with particle concentrations along the trajectories is a useful diagnostic approach for evaluating model behavior. It can highlight process-level differences between models and observations, especially when interpreted through the lens of known atmospheric physics. For instance, Khadir et al. (2023) showed that features in the correlation structure can be attributed to known physical processes — such as new particle formation (NPF), particle growth, or wet scavenging — even

https://doi.org/10.5194/egusphere-2025-2559
Preprint. Discussion started: 1 July 2025

when the correlation is not directly driven by precipitation itself. In this way, our physical understanding helps constrain the range of plausible drivers and potential confounders in the observed relationships.

However, separating confounders and process relationships can still be difficult, especially when dealing with many sources of data (multiple models and stations). Using correlations for model evaluation runs poses some risks in terms of interpretations: confounding factors may in some cases drive the correlation, and then the process under consideration may not be the one actually responsible for the observed agreement or disagreement. To complement the correlation-based analysis and account more systematically for potential confounding factors, we apply an XGBoost regression model (Chen and Guestrin, 2016) to predict particle concentrations based on a minimal set of meteorologically and chemically relevant predictors. The idea is to include core factors that may confound the results, like source regions (through trajectory position) and diurnal variability like boundary layer dynamics (through time of day).

One model is built for each data source (observations/reanalysis and models), for each station, and for each target variable. We present results for the target variables N_{10-30}, N_{50-100}, N_{100} and N_{200}, representing different aerosol size ranges. The model is thus trained to predict these particle concentrations. The input features include:

- 6-hour average trajectory position, converted to polar coordinates relative to the station and discretized to the nearest integer (i.e. r and θ for each 6-hour period).
- 6-hour average precipitation rate
- Time of day at the time of the PNSD measurement
- Day of year at the time of the PNSD measurement

The models are implemented using the Python package XGBoost (Chen and Guestrin, 2016), with squared error as the objective function, a tree method set to 'hist', learning rate of 0.1, maximum depth of 6, and 300 boosting rounds. In Supplement Sect. S13, we show leave-one-year-out validation results to assess model generalization performance.

2.7 Definitions and terminology for the analysis

The correlation analysis is performed separately for each season to avoid seasonal influence. The seasons are defined differently for each station according to their local climate, as presented in Table 2.

Number concentrations are analyzed and presented both as full size distribution in $dN/dlog_{10}(D)$ and concentrations in size intervals. For the latter, N_x is used to signify the particle number with diameter greater than $x\,\mathrm{nm}$, while N_{x-y} indicates the particle number with diameter larger than x but smaller than $y\,\mathrm{nm}$.

https://doi.org/10.5194/egusphere-2025-2559
Preprint. Discussion started: 1 July 2025

	Season	Months
Hyytiälä	DJF	Dec–Feb
	MAM	Mar–May
	JJA	Jun–Jul
	SON	Sep–Nov
Zeppelin	Haze	Mar–May
	Summer	Jun-Sep
	Slow-build up	Oct–Feb
ATTO	Wet	Feb–May
	Wet-to-Dry	Jun–Jul
	Dry-to-Wet	Dec–Jan
	Dry	Aug–Nov

Table 2. Months corresponding to each season

3 Results and discussion

3.1 Precipitation evaluation

Figure 2 shows normalized frequency of precipitation rate for the different stations. The leftmost panels shows the number of absolute zero values versus very low (below 0.05 mmh^{-1}) values. For ATTO, note that the satellite product used for the observations has fewer instances of low precipitation rate compared to the models, and has more higher values instead. This is likely because to the input data for the observations at ATTO have a resolution of 0.25 $\times$ 0.25 degrees, which is much higher resolution than the models have (typically more than 1 degree), and this will naturally lead to larger number of extreme values. For the 6 and 96 hour accumulated precipitation (see Figs. S2 and S1) the models and the observations are fairly comparable, except that ECHAM-SALSA has lower accumulated precipitation than the others at ATTO.

3.2 New particle formation and early growth

In this section, we focus on seasons where NPF is known to be a relevant process in each station: For Hyytiälä, we focus on spring (Dada et al., 2017), for Zeppelin we focus on the summer season (Lee et al., 2020), and for ATTO we focus on the wet season when nucleation mode particles have been frequently observed to be injected into the boundary layer via downdrafts (Franco et al., 2022).

Figures 3–5 show the correlations between the PNSD (diameter along the x-axis) and precipitation along the back trajectories (y-axis) for the stations during the seasons mentioned above (MAM for Hyytiälä, Summer for Zeppelin and Wet season for ATTO). An example on how to interpret this type of plot is: the negative correlation e.g. for particles larger than 100 nm for

https://doi.org/10.5194/egusphere-2025-2559
Preprint. Discussion started: 1 July 2025

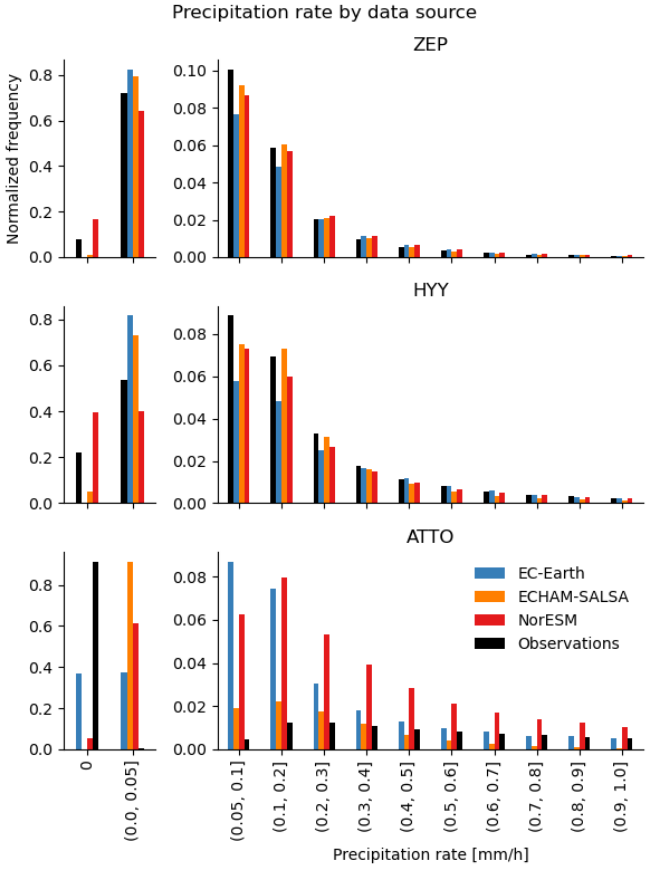

Figure 2. Frequency of precipitation rate [mm/h] along all trajectories.

precipitation rate further back in time than 30 hours (i.e. the upper right quadrant in each plot) indicates that precipitation at that time before arrival at the station is consistently associated with less particles in that size range measured at the station, i.e. if it rained heavily 40 hours ago, you would expect fewer particles than if it did not.

Hyytiälä: The observations (top left panel in Fig. 3) show a positive correlation with the smallest particles (below 20–50 nm) at around 30–65 h back in time. There is a further positive correlation with particles within the 50–100 nm size range with precipitation that took place at earlier, around 60-96 hours prior to the observation of the particles. We interpret these positive correlations as originating from NPF indirectly induced by past precipitation. Following this logic, the further into the past the precipitation occured, the larger the particles originating from this precipitation induced NPF have had time to grow, hence explaining why a positive correlation emerges between larger particles (50–100 nm) and precipitation that occurred a long time ago (90–96 h). Very recent precipitation (approximately 0–20 h), on the other hand, is seen to correlate negatively with the smallest particles (below 100 nm), which is consistent with NPF being inhibited by reduced photochemistry limiting oxidant availability to produce NPF precursors (e.g. Jokinen et al., 2017) in addition to a loss of critical NPF precursors such

https://doi.org/10.5194/egusphere-2025-2559
Preprint. Discussion started: 1 July 2025

as gas phase sulfuric acid and sulfur dioxide via wet and dry deposition. Moreover, a high condensation sink associated with rainfall and high humidity (swelling particles) may limit NPF during rainfall and we also expect direct scavenging of smaller particles by precipitation (e.g. Slinn, 1984).

All models show signs of NPF induced by past precipitation, though the timing differs. In terms of NPF inhibition by recent precipitation, ECHAM-SALSA and NorESM both have offline oxidant fields (read from file), which means that the effect of clouds (associated with recent precipitation) will not influence the oxidant availability and precursor production, except via wet/dry deposition of the precursors (mainly SO_2). This may explain why ECHAM-SALSA has no negative correlation with recent precipitation, and NorESM has a weaker correlation than what is observed. Also, NorESM has no explicit representation of nucleation mode particles, which means that the newly formed particles are put directly into the Aitken mode when they are formed (this can also be observed in the PNSD in Fig. 3). This, combined with wet scavenging of precursors probably also explains why there is still a weak negative correlation with recent precipitation in NorESM, despite the fact that the oxidants are the same regardless of precipitation.

EC-Earth, as opposed to the two other models, has online oxidant chemistry and should thus be able to represent the NPF inhibition due to cloudiness associated with recent precipitation. This is seen for the very smallest particles, but there is also a dominant positive correlation for particles larger than 10 nm which is likely unrelated to NPF, but rather related to the same process driving the positive blob in the bottom right corner in the observations. We discuss this below in Sect. 3.5. The negative correlation for the sub-10 nm particles in EC-Earth is consistent in timing with the observed NPF inhibition by recent precipitation, and is replaced by a positive correlation at around 30 hours back in time (again consistent with the observations).

In terms of the growth to larger sizes, which can be seen in the observations (see also Fig.1), none of the models exhibits significant positive correlations above 50 nm, with the extreme being EC-Earth which shows no positive correlations beyond 10 nm. This is of considerable importance because it suggests that the models (at least the ones in this study) in fact underestimate particle growth to CCN sizes. Note that when using the GDAS precipitation data from HYSPLIT, the particle growth is shown to even larger sizes in the observations (see Fig. S10).

Zeppelin: At Zeppelin, the observations in Fig. 4 similarly show positive correlations for particles between 10 and 40 nm and precipitation a bit earlier than 40 h back in time. There are also signs of growth up to above 50 nm at around 80 h back in time. The models on the other hand exhibit similar patterns to what is seen at Hyytiälä: ECHAM-SALSA shows positive correlations for the smallest particles even for recent precipitation, NorESM has negative correlations for recent precipitation across the range (likely again due to a lack of explicit representation of the smallest particles, which may in reality be less affected by nucleation scavenging), but positive correlations between the smallest range and precipitation more than 60 hours before arrival at the station. EC-Earth again has a surprising positive correlation with recent precipitation across the size range (from the smallest up to 130 nm), and contrary to Hyytiälä, it does not show signs of NPF inhibition for concurrent/very recent rain fall.

Similarly to Hyytiälä, none of the models reproduce the growth up to 50 nm and larger sizes seen in the observations for precipitation further back in time, with EC-Earth again being the weakest, showing essentially no sign of growth for the particles in the smallest sizes.

https://doi.org/10.5194/egusphere-2025-2559
Preprint. Discussion started: 1 July 2025

ATTO: As mentioned above, fine-mode particles at ATTO tend to appear in bursts connected to downdrafts, potentially injecting particles formed in the upper troposphere into the boundary layer (see discussion in the introduction). This is likely indeed why we see a positive correlation with concurrent/very recent precipitation in the observations in Fig. 5, followed by subsequent growth to the 50–100 nm range, and suggested potential growth to above 100 nm (though not significant). In general, one might not expect ESMs to represent this downdraft transport well, due to the (1) parameterized representation of convection as well as (2) potentially lacking representation of the nucleation mechanisms important in the upper troposphere in the regions (Curtius et al., 2024; Shen et al., 2024; Bardakov et al., 2024). However, we do see models showing positive correlations between very recent precipitation and the smallest particles in ATTO, contrary to what is seen at the other stations. It is not, however, entirely clear that the models are getting this right for the right reasons. In fact, the positive correlations between the smallest particles (sub 20 nm) with precipitation in the models at ATTO station may also be due to unrealistic boundary layer nucleation – at least EC-Earth and NorESM. Figure S25 shows that these models (NorESM and EC-Earth) frequently have NPF events at ATTO (judging by the formation rate in NorESM and the high concentration of sub-10 nm particles in EC-Earth), while ECHAM-SALSA is more realistic in terms of fewer boundary layer NPF events. For these models also the positive correlations only start for precipitation slightly back in time, while in the observations they are immediately connected to the precipitation. ECHAM-SALSA, on the other hand, has too few particles in the sub-50 nm range compared to the observations. Therefore, even if the downdraft transport were to be responsible for the positive correlations, it is clearly not strong enough; this could be due to either a lack of particles aloft or insufficient downward transport.

Note that all the models have diurnally oscillating pattern in the correlations at ATTO when going back in time. This originates from the diurnal pattern in the precipitation (Fig. S4 together with a diurnal pattern in the number concentrations (Figs. S5– S7). These are quite inaccurately represented in the models: The observations tend to show a relatively stable particle concentration for the larger particles (above 50 nm) with slightly lower concentrations during the night, while the models show the opposite. For the smallest particles (10-30 nm, the observations show a decrease during the day, while the models (except NorESM, which does not represent this range well), show a flatter pattern. It is beyond the scope of this study to explore the reasons for the models' failure in these regards, but it is likely related to the daytime mixing of the boundary layer with cleaner free tropospheric air.

To understand the overall effect of precipitation without the impact of the diurnal pattern, we show in Fig. 6 the correlations calculated using the daily mean in both PNSD and precipitation rate. We see that the features observed in the observational data and ECHAM-SALSA remain mostly unchanged. However, NorESM and EC-Earth now establish a potential link between the smaller particles and precipitation, accompanied with very rapid growth to larger sizes. In NorESM the particles seem to immediately grow to sizes larger than 50 nm, with some signs of growth to sizes above 100 nm (reduced negative correlation for precipitation further back in time). EC-Earth also shows signs of rapid growth (positive correlations with the Aitken and accumulation mode particles with recent precipitation), as well as potential growth with less recent precipitation in time. The negative correlations in between the Aitken and accumulation mode can likely be attributed to the modal structure of the model, where particles are moved to a larger mode once the inital mode grows large enough in median diameter. This very rapid growth is consistent with the findings of Blichner et al. (2024) in the ATTO environment: NorESM and EC-Earth overestimate

https://doi.org/10.5194/egusphere-2025-2559
Preprint. Discussion started: 1 July 2025

the amount of secondary organic aerosol in the ATTO environment. In addition, Blichner et al. (2024) also show that ECHAM-SALSA is more consistent with the observations in terms of organic aerosol at ATTO. However, the weak positive correlation in this model is rather due to the lack of particles than a lack of growth: since the model hardly has particles in the sub-50 nm range, it cannot not present a positive correlation.

Overall, with the analysis presented above, we cannot rule out that the models adequately represent the bursts of small particles associated with rainfall at ATTO. However, we can clearly show that in NorESM and EC-Earth, the growth to larger sizes is strongly overestimated, and for ECHAM-SALSA, the source is likely underrated.

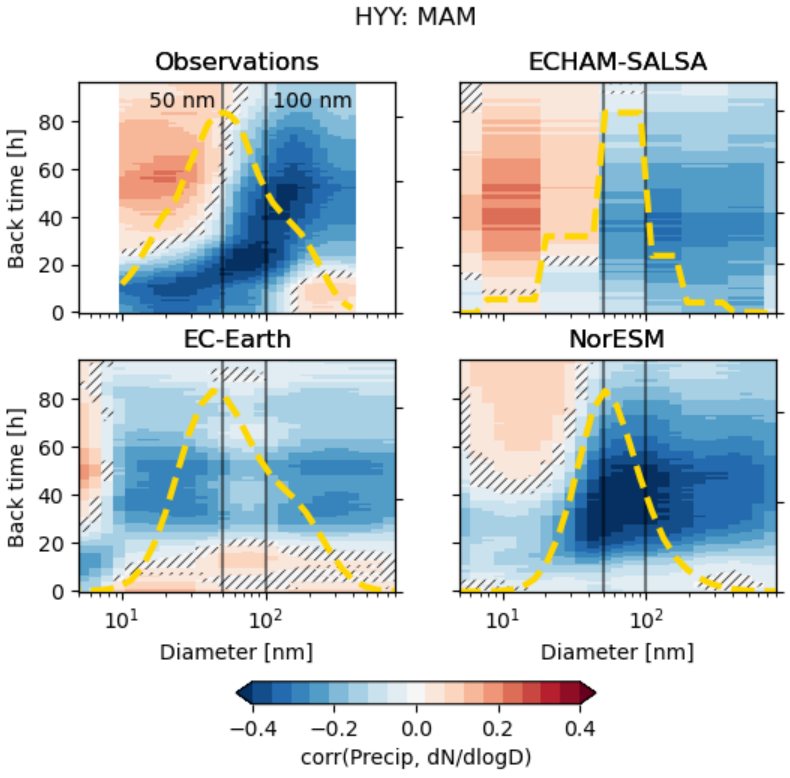

Figure 3. Correlation between precipitation rate and PNSD, MAM, Hyytiälä. The yellow lines show the shape of the PNSD during the same time period. Hatched areas indicate regions where the correlations are not statistically significant ($p > 0.05$).

3.3 Scavenging of particles

3.3.1 Nucleation and small Aitken mode

For the smallest particles, the scavenging is likely to be apparent only for very recent precipitation due to the short lifetime and indirect precipitation source of particles via NPF discussed above. Additionally, whatever relationship is observed, we see will be a combination of NPF inhibition by reduced photochemistry associated with cloudy conditions and wet scavenging

https://doi.org/10.5194/egusphere-2025-2559
Preprint. Discussion started: 1 July 2025

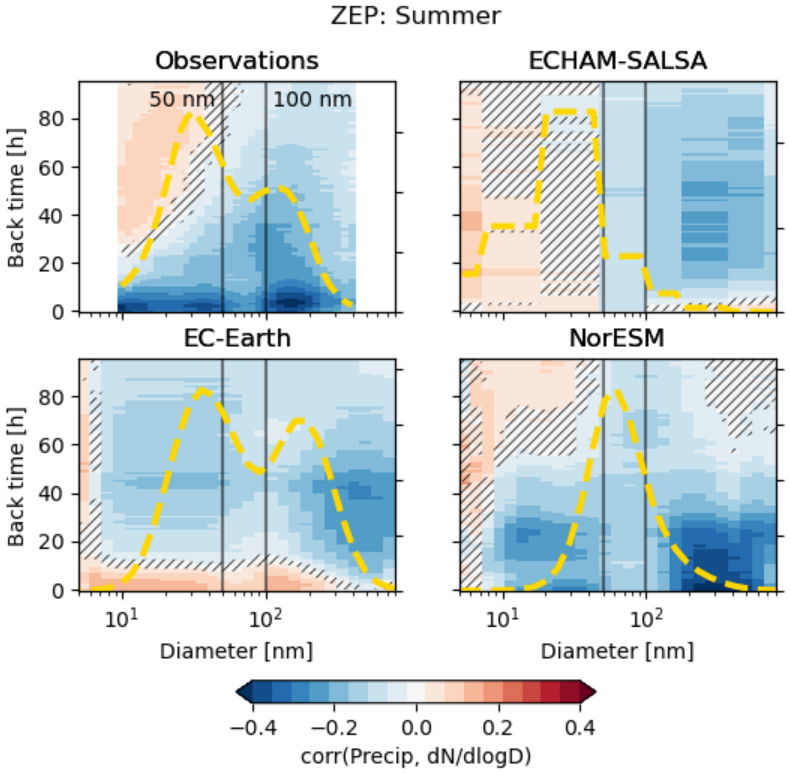

Figure 4. Correlation precipitation rate rainfall and PNSD, Summer, Zeppelin. The yellow lines show the shape of the PNSD during the same time period. Hatched areas indicate regions where the correlations are not statistically significant ($p > 0.05$).

of NPF precursor gases and finally direct scavenging of the particles. As mentioned, NorESM and ECHAM-SALSA have offline oxidant chemistry, meaning that the oxidant concentration is read from monthly mean files with an imposed diurnal variability on top of it. This means that the cloud cover has no impact on the photochemistry in these models and they could therefore produce NPF even during cloudy conditions. This is likely the reason why these models in general have a too weak negative correlation for recent precipitation (see Figs. 3–5 and Figs. S9b,S11b,S12b,S13b,S14b, S15b). On the other hand, all the models represent the wet removal of NPF precursor gases (sulfur dioxide, gas phase sulfuric acid, organics, etc.), which is effective if the grid box is in the cloud or affected by precipitation. To separate the impact of NPF inhibition from impact of scavenging of the smallest particles, one approach is to investigate the impact of precipitation during night time, as NPF is very rare during night, especially with subsequent growth. This is shown in Fig. 7 which has N_{10-30} binned by recent (6 h) accumulated precipitation and separated into night time (defined as between 21:00 and 03:00) and all data. The night-time conditions additionally have a requirement that 6 h accumulated radiation is below $30 \mathrm{W m^{-2}}$.

At Zeppelin, the reduction in N_{10-30} with increased 6 h accumulated precipitation is weaker for night-time than for for all values. This may be expected because during the day, we expect both the NPF inhibition and the direct wet deposition loss

https://doi.org/10.5194/egusphere-2025-2559
Preprint. Discussion started: 1 July 2025

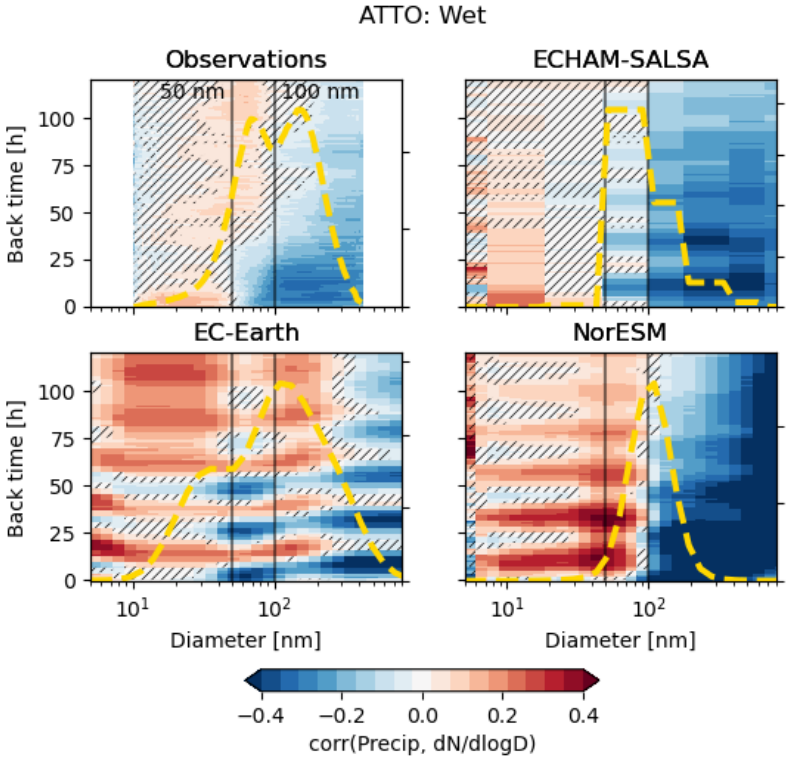

Figure 5. Correlation between precipitation rate and PNSD, Wet season, ATTO. The yellow lines show the shape of the PNSD during the same time period. Hatched areas indicate regions where the correlations are not statistically significant ($p > 0.05$).

processes to be at play, while during night, NPF inhibition is expected to be minimal, because anyway there is little to no NPF. ECHAM-SALSA seems to do better during night, where we see a reduction in N_{10-30}, rather than the slight increase observed when sunlit hours were included. NorESM on the other hand, remains unchanged, indicating – in consistence with Fig. 4 – that there is little influence of NPF here. EC-Earth has increasing N_{10-30} with increasing recent precipitation independent of whether it's night or all data – again, consistent with the unrealistic positive correlations for recent precipitation in Fig. 4.

For Hyytiälä, the reduction in N_{10-30} is similar between night and all data in the observations, though a little stronger during night. This is somewhat surprising given that, as mentioned above, during the day, both NPF inhibition and direct wet deposition are expected to reduce N_{10-30} with increased precipitation. Therefore, we would have expected the signal to be stronger for all data than for night only. NorESM is clearly closer to the observations for the night-time values, indicating that NPF plays a role in the weak negative correlation in Fig. 3 between recent precipitation and N_{10-30} particles in NorESM. However, for both ECHAM-SALSA and EC-Earth the pattern is opposite, with night time values showing a more positive relationship with increased 6 h accumulated precipitation. These are thus likely not NPF related, but rather related to the overall positive correlations for mass and number discussed below in Sect. 3.5.

https://doi.org/10.5194/egusphere-2025-2559
Preprint. Discussion started: 1 July 2025

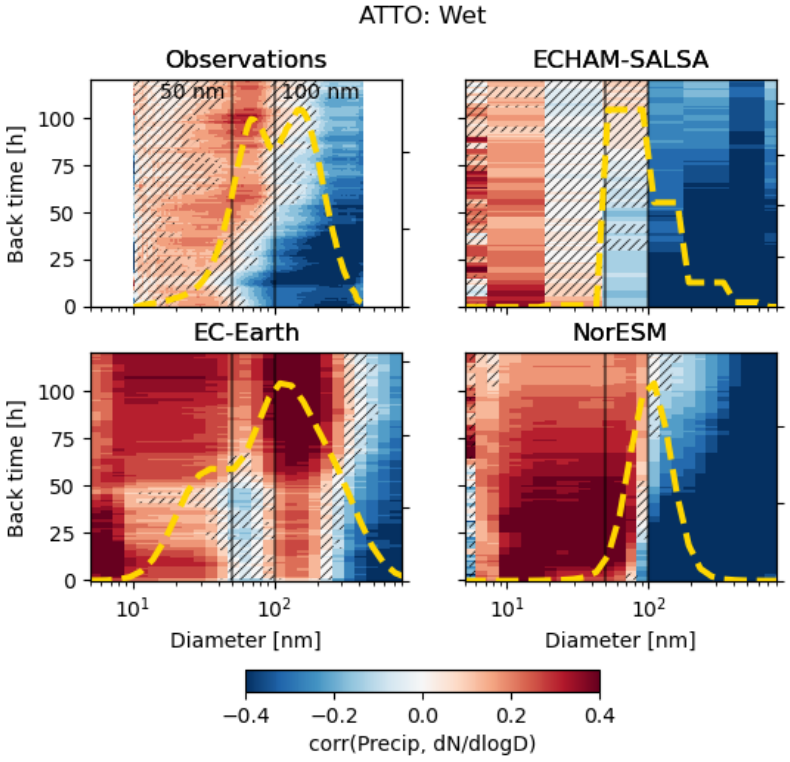

Figure 6. Correlation between precipitation rate and PNSD using daily mean values form both the PNSD and the precipitation, Wet season, ATTO. The yellow lines show the shape of the PNSD during the same time period.

Lastly, for ATTO, we do not necessarily expect a change between night and day if the appearance of the smallest particles is not related to photochemically induced NPF, but rather to downdrafts. However, convection typically happens during the late afternoon and evening (Machado et al., 2024), and one might then expect less of it during night. This is in fact what we see, with decreases for the first 4 bins of accumulated precip during night, and then an increase for the highest precipitation bins (potentially indicating convective precipitation). For the full dataset, however, we see an increase in N_{10-30} with increasing precipitation. ECHAM-SALSA and NorESM both have positive relationships for the night-time values. NorESM has more of a zero influence for the full dataset, while ECHAM-SALSA has a very high relative increase with increasing accumulated precipitation (likely related to very low particle number concentration). EC-Earth has very weak impact of precipitation on N_{10-30} at ATTO independent of the time of day.

It is hard to draw conclusions about model skill from these findings, though at least for EC-Earth, it seems like direct scavenging is not strong enough at any of the stations. From the ATTO results, they seem to indicate that the positive relationships between N_{10-30} and recent rainfall in NorESM and EC-Earth are not in fact highly related to local NPF, because if they were there would be a clearer difference between night and all values.

https://doi.org/10.5194/egusphere-2025-2559
Preprint. Discussion started: 1 July 2025

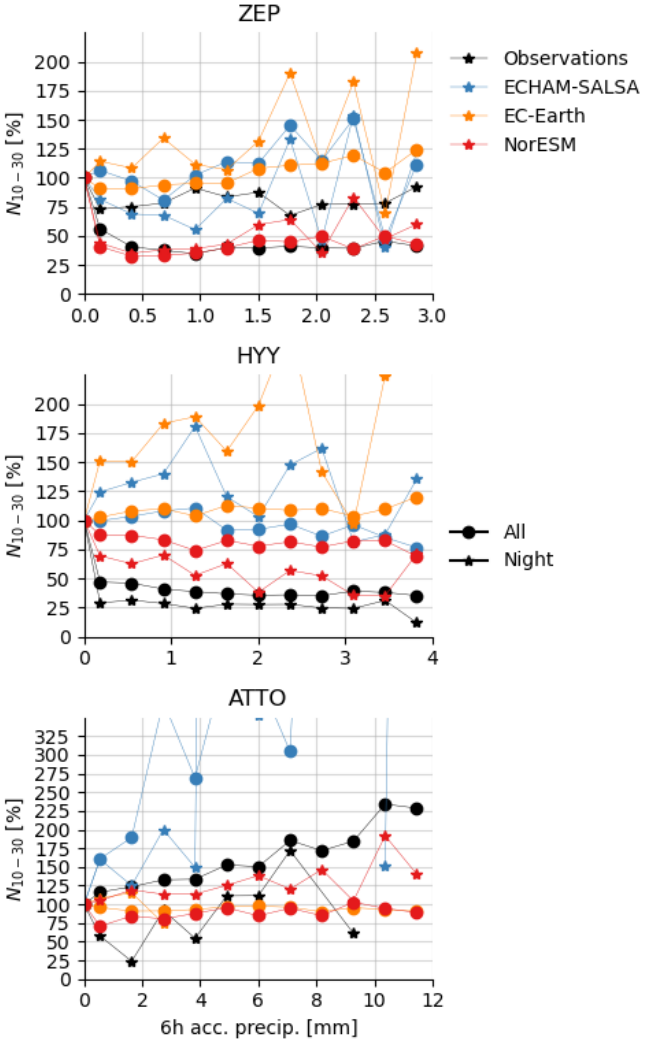

Figure 7. N_{10-30} binned by recent (6 h) accumulated precipitation. The dataset is divided into all data and only night time values (defined as between 21:00 and 03:00 plus accumulated radiation below 30 Wm^{-2}).

3.3.2 Accumulation mode and large Aitken mode particles

Figures 8a and 8b show the correlations between N_{100} and N_{200} and precipitation along the back trajectories (see also e.g. Fig. 3,5 and S22,S21, S9b, S11b, S12b). Overall, one can here see that the observations seem to follow a similar pattern for all seasons at the same station and even somewhat between the stations, the models behave less consistently. For example, at the same station, the models exhibit quite different correlations depending on the seasons.

https://doi.org/10.5194/egusphere-2025-2559
Preprint. Discussion started: 1 July 2025

For Hyytiälä, the models mostly seem to agree well with the observations (Fig. 8a and 8b), with all of them showing a less negative or even positive correlation for recent precipitation (see discussion below in Sect. 3.5) and a strongly negative correlation for less recent precipitation (older than 24 h).

For Zeppelin, two seasons (Slow-build up and Haze) show zero or even somewhat positive correlations with precipitation between 24 and 72 h back in time. These positive correlations do not show up when using precipitation output from the GDAS reanalysis dataset via HYSPLIT (see Khadir et al. (2023) or Figs. S14a and S15a), and therefore care should be taken in interpreting them. However, also when using precipitation from GDAS, the correlations are only weakly negative for these particular months (see Fig. S14 and S15). For these same seasons, EC-Earth has positive correlations for the whole size range (Slow build-up and Haze, see Fig. S14b and S15b) and NorESM has a very weak negative correlation for Slow build-up. It is noteworthy that these weak and positive correlations only occur during the cold months and in the Arctic. This could be related to the wet deposition efficiency of snow versus rain, though it could of course also simply be due to lower quality in the re-analysis products during this time. See discussion on the impact of temperature below in Sect. 3.4.

For ATTO, the observations show negative correlations for all the seasons – in particular in the Wet and the Wet-to-Dry season have strong negative correlations (bottom two lines in Figs. 8a and 8b). ECHAM-SALSA does best amongst the models here, when compared to observations, with only a slightly too strong negative correlation with precipitation. EC-Earth and NorESM have very strong oscillations in their patterns, likely caused by the diurnal pattern in their particle concentrations (discussed above, see Fig. S7 and S8). For NorESM, the correlation is highly season dependent here, with a highly negative correlation during the Wet season (see also Figs. 6 and 5) and the Dry-to-Wet seaons (see Fig. S22), but a positive correlation for the two other seasons. The pattern that appears when displaying the correlations for the full PNSD and precipitation (Figs. S20 and S21) is consistent with the main mode shifting in size to larger sizes in response to rain (negative correlations for smaller particles, positive for larger). This may happen when a reduction in number of larger particles and thus condensation sink, leads to increased growth of the remaining particles in the model and is likely what we see in NorESM here. The way that NorESM is set-up, this could happen instantaneously because the condensate is redistributed on the PNSD in each time step (no memory of where it was in the previous time step) (Kirkevåg et al., 2018). For EC-Earth, it is likely a similar phenomena with decreasing particle number leading to increased growth of the remaining particles (though in this model the condensate is not redistributed in each time step, so some time lag is expected). This is especially true for the Dry-to-Wet season, where there are only negative correlations for particles in the 10-50 nm range, but still positive correlations for the 50-200 nm range (Figs. S22). The fact that ECHAM-SALSA does not have these unrealistic (compared to the observations) positive correlations for larger particles at ATTO points to this being an issue with the modal structure of the aerosol parameterization in NorESM and EC-Earth, which ECHAM-SALSA, being a sectional scheme, does not suffer from.

To summarize, ECHAM-SALSA may be said to do the best in general, with the exception of recent precipitation at Zeppelin, which shows an unrealistic upturn in correlation. In general, NorESM can be said to more sensitive to season and station than what the observations suggest and has a particularly unphysical response to rainfall in ATTO due to the modal structure and the growth treatment. EC-Earth does well at Hyytiälä, but has a strong oscillation pattern at both ATTO and somewhat at

https://doi.org/10.5194/egusphere-2025-2559
Preprint. Discussion started: 1 July 2025

Hyytiälä. It also stands out with a significant positive correlations for the cold seasons at Zeppelin for the whole size range (see discussion below in Sect. 3.4).

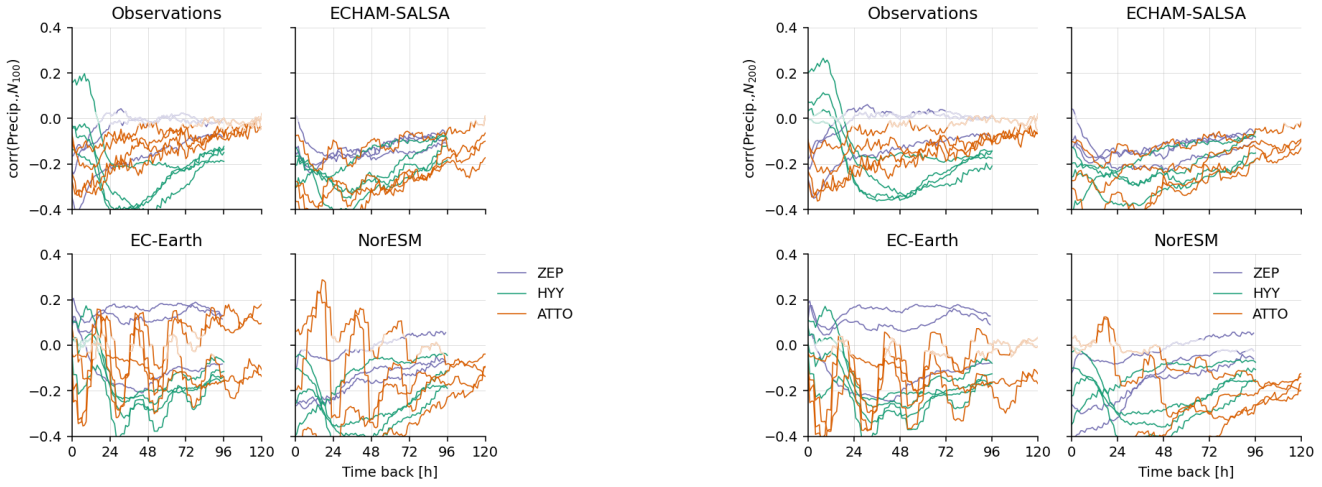

(a) N_{100} (b) N_{200}

Figure 8. Spearman correlations between precipitation rate and (a) N_{100} and (b) N_{200} for observations (top left) and models. Each line represents a season at a station.

3.4 Impact of temperature: indications for cloud phase

As shown in the section above, for Zeppelin, EC-Earth shows a surprising positive correlation between almost all particle size ranges and precipitation, and the only negative correlation is found during summer. Calculating separate correlations for cold (below -5 °C) and warm (above 0 °C) conditions at the stations, shown in Fig. 9, gives indications that cold conditions, and thus likely solid precipitation, are responsible for this positive correlation. Also, when separating the data into cold and warm periods, it becomes clear that the models agree with observations much better in the warm periods, with quite consistent negative correlations for recent precipitation at Zeppelin, and for not so recent precipitation in Hyytiälä. However, for the cold periods, the observations at Zeppelin do not show significant correlations, EC-Earth shows a positive correlation and NorESM displays fairly chaotic behaviour. ECHAM-SALSA is, on the other hand, exactly the same in the cold and the warm period, suggesting precipitation phase has of little importance in this model.

For EC-Earth the difference in the correlations between cold and warm aligns well with a very low in-cloud scavenging for ice and mixed phase clouds (see Tab. 1) compared to liquid clouds. When separating to cold and warm periods, EC-Earth actually turns out to be among the best-performing models for N_{100}.

https://doi.org/10.5194/egusphere-2025-2559
Preprint. Discussion started: 1 July 2025

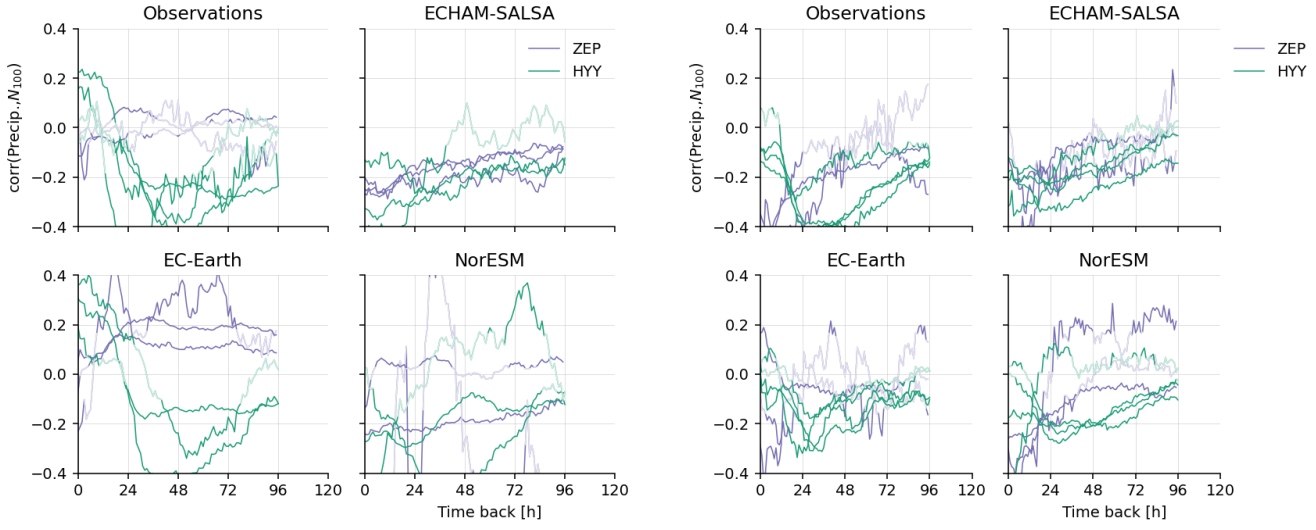

(a) Cold conditions: Temperature below -5 °C.

(b) Warm conditions: Temperature above 0 °C.

Figure 9. Same as Fig. 8b but for N_{100} and for cold versus warm conditions at the station separately.

3.5 Cloud processing at Hyytiälä?

In Hyytiälä, the observations show that the negative correlation between precipitation and accumulation mode particles tends to have a maximum in negative correlation 20-40 hours back in time followed by a positive correlation for recent precipitation (Observations in DJF, MAM, JJA and almost in SON, see Figs. 3, S9b, S11b, S12b). This is partially reproduced in the models: EC-Earth has a positive correlation in DJF, MAM and SON, NorESM only almost has one in MAM but with an almost zero correlation in JJA, ECHAM-SALSA only has a weakened negative correlation for MAM, JJA and SON). Khadir et al. (2023) suggest that this positive signal may be due to cloud processing.

However, when analysing the observed composition of the particles and how this correlates with precipitation at Hyytiälä (see Fig. 10), it seems that most compounds have a positive correlation with recent precipitation. Typical cloud processing products like sulfate do not stand out in this regard, but rather look similar to eBC, organics and NO_3. The models tend to produce a similar pattern: the correlation moves to less negative or even positive for recent precipitation for all species except for sea salt (SS), which does the opposite. Overall, this suggests that both models and observations may be capturing some spurious correlation between source regions and precipitation, since the pattern shows up both for species that may indicate cloud processing and ones that are unlikely to be positively influenced by cloud processing (for example BC). It also does not show up for SS, which is non-anthropogenic in origin.

Furthermore, dividing the trajectories into ones with both low recent precipitation (last 18 hours before the airmass arrival at the station) and low N_{200} (defined as below the mean) and high recent precipitation and high N_{200} (defined as above the mean) reveals a distinct spatial pattern (Fig. S26) where the first group comes from the north-west and the second comes from

https://doi.org/10.5194/egusphere-2025-2559
Preprint. Discussion started: 1 July 2025

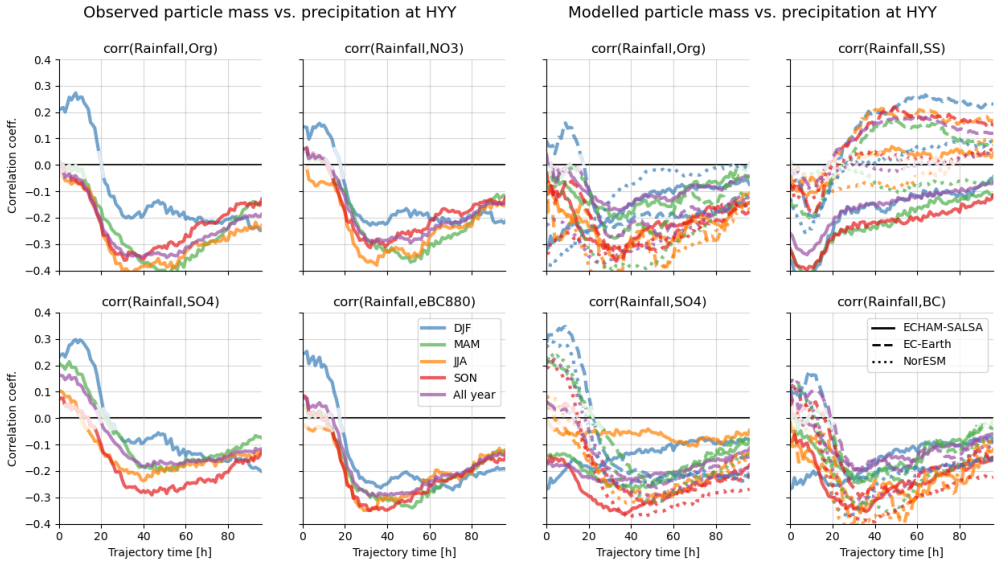

Figure 10. Correlations between precipitation rate and aerosol mass for observation (ACSM data) and models.

the south-east. This adds evidence to the spurious correlation claim. Restricting the data to the "polluted sector" (-175 to 5 degrees centered at the station) does also remove the positive correlation (see Fig. S29), however it is still there when restricted to the "clean sector" (see Fig. S30). This points to some difficulty when interpreting especially recent precipitation influence, because the impact of local sources is naturally higher. In the end, the evidence above is not completely conclusive as to what causes this positive correlation, but does suggest that it cannot be explained solely by a classic cloud processing in the sense of in-cloud sulfate production and droplet collision coalescence.

3.6 A second perspective: Using machine learning (XGBoost)

Finally, we also investigated the relationship between precipitation and the PNSD using a machine learning algorithm XGBoost (see methods in Sect. 2.6). This gives a valuable second perspective as the XGBoost regression we built also takes the trajectory positions, time of day and day of year as input. All these variables may be confounding factors for the relationships we observe. Furthermore, in the best case scenario, the XGBoost regression for each model will make it possible to exclude other potential errors the model might have from the analysis (they would be accounted for by other features) and focus on the process under investigation (here precipitation impact).

In Sect. S13 in the supplement, we present evaluations of the XGBoost model trained on the years up to 2018, and tested on year 2018. It reveals essentially that overall XGBoost captures the main features, but that the smallest particles are the hardest to predict. This applies especially for ATTO where XGBoost struggles to reproduce both models (except NorESM) and observations for N_{10-30}, and that Zeppelin is in general hard to predict with the input parameters chosen here. Section S12

https://doi.org/10.5194/egusphere-2025-2559
Preprint. Discussion started: 1 July 2025

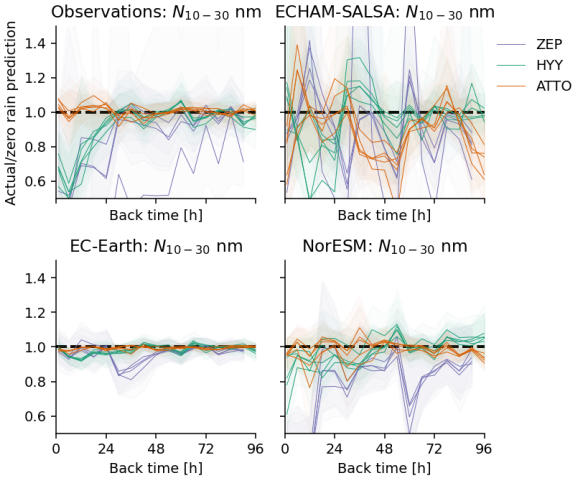

(a) N_{10-30}

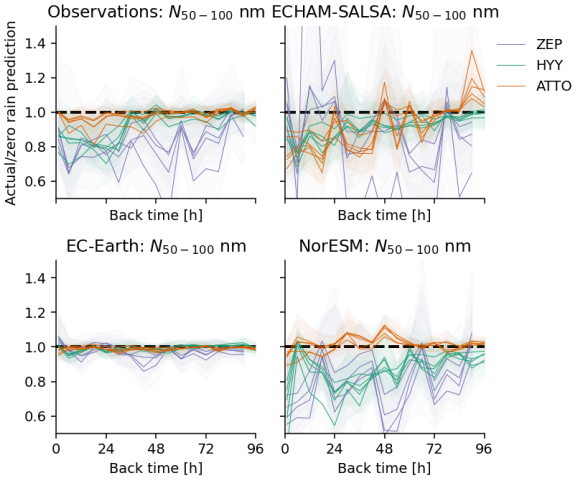

(b) N_{50-100}

Figure 11. XGBoost predicted N_{10-30} and N_{50-100} ratio between the using the actual rain along the back trajectories and the prediction when the rain was set to zero at each 6 hour interval back in time separately. Each line represents a season at each station.

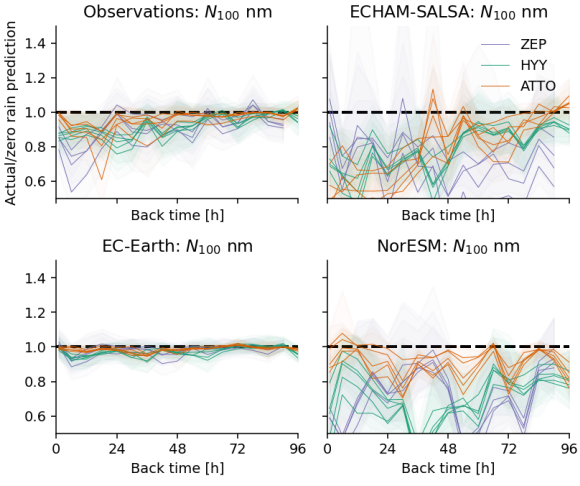

(a) N_{100}

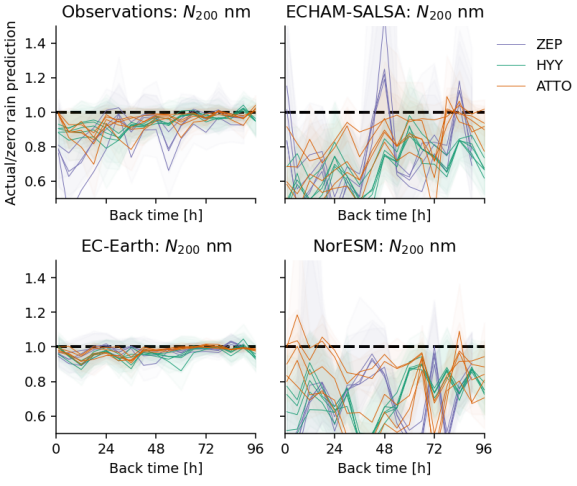

(b) N_{200}

Figure 12. XGBoost predicted N_{100} and N_{200} ratio between the using the actual rain along the back trajectories and the prediction when the rain was set to zero at each 6 hour interval back in time separately. Each line represents a season at each station.

also presents SHAP (SHapley Additive exPlanations) values for the XGBoost regression models (Shapley, 1953; Lundberg and Lee, 2017). SHAP values are a method from game theory used to explain the output of machine learning models. Essentially, these values explain how much each feature (i.e. our input parameters) contributed to a particular prediction.

https://doi.org/10.5194/egusphere-2025-2559
Preprint. Discussion started: 1 July 2025

Figure 11a shows the XGboost predicted precipitation impact on N_{10-30} as indicated by the ratio of predicted N_{10-30} with the actual precipitation in the model/re-analysis divided by the XGBoost prediction if precipitation was set to zero for each period back in time, individually. In other words, it shows a positive signal if the "real precipitation" caused an increase in N_{10-30} according to XGBoost, and a negative signal if it caused a decrease. The mean difference is calculated excluding cases where the precipitation is less than 0.05 $\mathrm{mm/h}$. This plot shows that for recent precipitation, XGBoost predicts a large decrease for Hyytiälä and Zeppelin in N_{10-30} due to precipitation, while predicting a small increase for ATTO, thus aligning with the relationships shown in Figs. 3–5 for the smallest particles. The models, in general, do not manage to reproduce this, except that they all agree about the small increase at ATTO. This is again consistent with models not reproducing NPF inhibition by clouds and precipitation, but could also indicate a too weak below-cloud scavenging of these particles. SHAP values for recent precipitation rates in Fig. S57, S58 and 13 show that 1) ATTO stands out in that XGBoost predicts higher N_{10-30} for high precipitation rates for all data sources and 2) that there seems to be a pattern of more moderate precipitation rates causing a decrease in N_{10-30} followed by an increase for strong precipitation. Note however that the XGBoost does quite poorly in predicting N_{10-30} at ATTO for all data sources except NorESM. These results should therefore be interpreted with some caution. If we assume that XGBoost is here picking up real features, however, then it adds to the evidence that models are in fact reproducing a downdraft transport of smaller particles associated with strong convective rainfall, in consistence with the the correlation results above (e.g. Fig. 5).

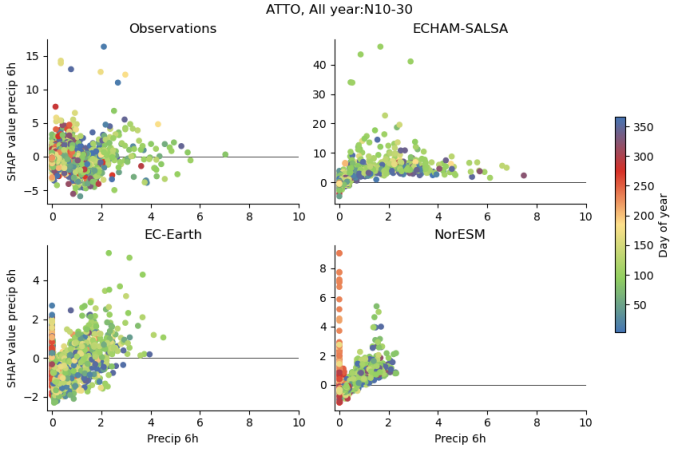

Figure 13. ATTO: Scatter plots showing the SHAP values for of the first 6h average precipitation rate prior to the airmass reaching the station for predicting N_{10-30}. The color indicated the day of the year.

EC-Earth stands out in all size ranges as having a very weak impact of precipitation on particle number in the XGBoost analysis. This is in spite of EC-Earth apparently being the easiest data source for XGBoost to replicate judging by the r-values in Fig. S68. The EC-Earth number concentration seems to be very predictable mainly by source region (see Sect. S12. From the correlation analysis, EC-Earth stands out as having strongly oscillating correlations at ATTO and positive correlations between precipitation and particle concentrations in the cold season in Zeppelin (see e.g. 8a). Also, somewhat

https://doi.org/10.5194/egusphere-2025-2559
Preprint. Discussion started: 1 July 2025

weaker negative correlations for EC-Earth than the other models can be seen for Hyytiälä for N_{100} and N_{200} (see Fig. 8a and 8b). Thus, combining these together, it is not completely unplausible that EC-Earth has a weaker impact of precipitation on aerosol number than the other models or what is observed. It is also the only one among the models that uses fixed scavenging coefficients for nucleation and impaction scavenging even in liquid clouds, which could explain why it behave differently from the other models.

The correlation analysis indicated that all the models underestimate the impact or growth of newly formed particles to sizes larger than 50 and 100 nm (except for NorESM and EC-Earth at ATTO, see Figs. 3– 6).The XGBoost analysis largely confirms this. For observations, recent precipitation (less than 24 h) at Zeppelin and Hyytiälä has negative impact on N_{10-30}, turning to a weakly positive impact for precipitation more than 24 hours back in time, while in ATTO it is weakly positive (Fig. 11a) from the very recent precipitaton. For N_{50-100} XGBoost indicates a net zero or weakly positive impact of precipitation around 48 h back in time for ATTO and Hyytiälä, but for Zeppelin it approaches zero around 80 h back in time (again consistent with e.g. Fig. 4. For N_{100} (Fig 12a) the negative impact of precipitation persists for longer (around 72–8 h). The models on the other hand, do not show signs of growing NPF particles in the same way for Hyytiälä and Zeppelin: both ECHAM-SALSA and NorESM have the impact of precipitation on N_{50-100} (Fig. 11b) consistently negative back in time, not returning to net zero for older precipitation as seen in the observations. EC-Earth has weak impact all over. At ATTO, as seen in the correlation plots, NorESM shows positive impact of precipitation on N_{50-100} for precipitation between 0 and 72 h back in time, while for ECHAM-SALSA it only approches net zero around 38 h back in time. NorESM has a negative impact of precipitation on N_{100} for all stations that is fairly constant with back time, which is likely because the particles cannot grow larger in the aerosol scheme in NorESM (see e.g. Blichner et al., 2021). An exception is a slight positive impact for 6 h at ATTO. For N_{50-100} at ATTO station, NorESM also with this approach shows a increase in N_{50-100} with precipitation almost immidiately. This indicates that the model has both too fast and too slow growth: As shown in Blichner et al. (2024), NorESM has too much high production of biogenic SOA in the ATTO region, consistent with too fast growth to sizes above 50 nm. However, the aerosol scheme in NorESM does not represent growth out of the Aitken mode, meaning that growth can only shift the whole mode to larger sizes, thus efficiently constraining growth to larger sizes (see e.g. discussion in Blichner et al., 2021).

For Zeppelin, EC-Earth has positive correlations between precipitation and N_{50-100} and N_{100} (Figs. 11b and 12a), which XGBoost does not predict (see also SHAP values for recent precipitation in Figs. S59 and S62). For Hyytiälä, EC-Earth actually seems to correspond quite well with the observed for N_{100} (which it also did for the correlations), while for N_{50-100} it is almost always close to zero.

Overall, one could argue that ECHAM-SALSA is the most accurate for N_{50-100} and N_{100}, with signs of a return to zero for both N_{50-100} and N_{100} with older precipitation at Hyytiälä – although too weak – and an even positive impact at ATTO. The correlation plots show positive values between recent (less than 6 h) precipitation and N_{100} or N_{200} (see Figs. 8a and 8b) for models and the observations at Hyytiälä. The XGBoost results does not suggest a positive here (see Figs. 12a and 12b) for any of the models or the observations. Instead XGBoost likely attributes the positive correlation to source region. This gives further evidence that it is indeed a spurious correlation between precipitation and source region, rather than a real process related to cloud processing.

https://doi.org/10.5194/egusphere-2025-2559
Preprint. Discussion started: 1 July 2025

4 Conclusions

In this study, the timing-resolved impact of precipitation on PNSD is investigated in models versus observations – in other words, what is the impact of precipitation at different times in the past on particles in different parts of the size range (Khadir et al., 2023). This is done for three stations: Zeppelin in the Arctic, Hyytiälä in the boreal forest, and ATTO in the Amazon rain forest.

The objective of this is to evaluate the impact of precipitation on the CCN budget, which again impacts cloud properties and local temperature and climate. We have evaluated three GCMs, NorESM, EC-Earth and ECHAM-SALSA, using primarily the methodology developed by Khadir et al. (2023), where the correlation between precipitation rates along back trajectories and observed (or modeled) PNSD at the stations are utilized. We supplement this analysis by using an XGBoost regression model for each data source (models and observations) trained to predict particle concentrations based on a minimal set of meteorologically and chemically relevant predictors, including precipitation rate, trajectory position, time of day, and day of year. We then examine the impact of precipitation predicted by the XGBoost model for each data source in order to be able to account for potentially confounding factors.

A key goal was to investigate to what extent the models could represent the indirect source of NPF induced by precipitation identified in (Khadir et al., 2023), that is, there is a positive correlation in the observations between precipitation several days back in time and particles of the smallest sizes, likely originating from growing particles formed by NPF. The mechanism that causes this is hypothesized to be lower condensation and coagulation sink due to precipitation, priming the atmosphere for NPF. We see that models tend to represent the positive correlation between precipitation in the past and smaller particles. However, for Zeppelin and Hyytiälä, the positive correlation is less strong than in the observations and also does not extend to as large sizes as in the observations. This indicates that the growth of the newly formed particles is too slow in the models or that the number of particles formed is not enough to induce a positive correlation for particles in CCN sizes (above 50 nm).

ATTO stands out from the other two stations with respect to NPF, because the correlation between rainfall and small particles is immediate, i.e. there is a positive correlation even for rainfall just before arriving at the station (recent rainfall). This has been hypothesized to be driven by downdraft transport of particles during strong convection (Wang et al., 2016) or by injection of ozone by downdrafts (Machado et al., 2024). Our initial hypothesis was that the models would not be able to represent this, due to their coarse resolution and the simplified representation of downdrafts. However, the models do show an almost immediate positive correlation between recent precipitation and small Aitken/nucleation mode particles. The question remains if they have it right for the right reasons: Both EC-Earth and NorESM have local nucleation at ATTO, which has been believed to not occur (see e.g. Wang et al., 2016), so they may instead represent positive correlations due to these. On the other hand, both models clearly respond differently to recent precipitation at ATTO compared to at Zeppelin and Hyytiälä: at the former there is a positive correlation with recent precipitation, and the latter the positive correlation is only for precipitation a day or more in the past. This is also supported by the XGBoost analysis. Furthermore, if the appearance of the smallest particlethe NPF after rain is driven by ozone injection with downdraft (Machado et al., 2024), then NorESM and ECHAM-SALSA certainly cannot represent these injections and must be representing the positive association for a different reason.

https://doi.org/10.5194/egusphere-2025-2559
Preprint. Discussion started: 1 July 2025

Overall, this seems to suggest that models and observations agree that rain correlates with the appearance of smaller particles at ATTO, and this should be further investigated both in terms of whether the models are right for the right reasons and in terms of what the models can tell us about the real mechanism behind the appearance of these particles at ATTO.

Both EC-Earth and NorESM show positive correlations with recent precipitation for very large particles at ATTO. This suggests a much too fast growth of newly formed particles in these models, consistent with the overestimation of organic aerosol found in these models in (Blichner et al., 2024). It also may suggest challenges with these models' modal structure, giving increases in much too large large particles due to the limited resolution in size and highly parameterized growth.

In terms of particle scavenging, the results were inconclusive for the smallest particles (10–30 nm), although the models did seem to consistently underestimate the scavenging at Hyytiälä, which was also shown in the XGBoost results. For accumulation mode particles (N_{100} and N_{200}) models mostly agree well with observations for Hyytiälä. For ATTO, ECHAM-SALSA performs fairly well, but the two other models struggle due to highly unrealistic growth of the newly formed particles (see above) and therefore have positive correlation even for N_{100} and N_{200}.

For Zeppelin, there are considerable discrepancies in the cold seasons. Note that using different re-analysis datasets for the precipitation (GDAS versus ERA5) here also made a larger difference than in the other stations, and caution should therefore be advised in interpreting the results. This is perhaps not surprising, given the wide discrepancies in cloud properties among reanalysis datasets in the Arctic in general (Yeo et al., 2022). However, it is clear that when the data are separated into times with temperatures below -5 °C and above 0 °C, the models do much better when temperatures are above 0 degrees, indicating that the discrepancies originate from cold clouds and the treatment of mixed and glaciated clouds. Note that even the observations do not show a significant negative correlation between N_{100} and recent precipitation at Zeppelin. ECHAM-SALSA shows similar results for cold and warm periods, which is actually inconsistent with the observations at Zeppelin, which show much stronger negative correlations when temperatures are higher.

Finally, the XGBoost results mainly align with the correlation analysis, thus strengthening our confidence in the conclusions. In particular, the correlation plots show positive correlations between recent precipitation and N_{100} and N_{200} at Hyytiälä, something that was hypothesised in Khadir et al. (2023) to be due to cloud processing. The XGBoost results, on the other hand, do not attribute this to precipitation but rather source region. This demonstrates how using machine learning used like this in model evaluation can serve as a powerful tool for uncovering potential spurious correlations and to control for factors unrelated to the process under investigation.

Code and data availability. The analysis code will be made available via Github+Zenodo before final publication, but can currently be found here: https://github.com/sarambl/PRCP2SZDST.git. The particle number size distribution and trajectory data used in this study are available to download at https://doi.org/10.5281/ZENODO.7907473 (Khadir, 2023), which also includes the precipitation data from TRMM 3B42 V7 satellite product (Michot et al., 2018) used for ATTO. The temperature timeseries can be downloaded from ACTRIS for Zeppelin (Aas, 2015, 2016, 2021b, a, 2022) and Hyytiälä (Kulmala and Petäjä, 2024). The aerosol particle composition data from the ACSM and the eBC data from Aethalometer measurements for Hyytiälä is available from the EBAS database at ebas-data.nilu.no. ERA5 data is available

https://doi.org/10.5194/egusphere-2025-2559
Preprint. Discussion started: 1 July 2025

for download from https://doi.org/10.24381/CDS.ADBB2D47 (C3S, 2018). The full dataset for the analysis is available to download from https://doi.org/10.5281/zenodo.15528150 (Blichner, 2025).

Author contributions. SB did the analysis and wrote the paper with help especially from IR, TK and ST. CS, SB and IM ran the models (EC-Earth, NorESM and ECHAM-SALSA respectively). SB, TK, ST and IR conseptualized the study. AV especially gave input and support on the XGBoost analysis. All co-authors commented, edited and gave feedback on the manuscript.

Competing interests. Some authors are members of the editorial board of ACP.

Acknowledgements. We acknowledge funding from the European Commission grants INTEGRATE no. 867599 (IR, SB, LH, TK), CERTAINTY (Cloud-aERosol inTeractions & their impActs IN The earth sYstem) no. 101137680 (IR, SB, TvN, MI, HK), the Swedish Research Council grant no. 2023-03842 (SB), and grant no. 2022-02836 (CS), Knut and Alice Wallenberg Foundation grants AtmoRemove no. 2015.0162 (IR, LH, TK), AtmoCLOUD no. 2021.0169 and no. 2021.0298 (IR, LH, TK), and CLIVE no. 2022.0104 (IR, LH, ST, RK) and Goran Gustafssons stiftelse (IR).

The computations and data processing were enabled by resources provided by the National Academic Infrastructure for Supercomputing in Sweden (NAISS) at at the National Supercomputer Centre (NSC), partially funded by the Swedish Research Council through grant agreement no. 2022-06725.

Further, we acknowledge Krista Luoma for valuable help with the black carbon data and Peter Tunved for great discussion and input. Thanks also to Diego Aliaga for always providing good discussions and input.

https://doi.org/10.5194/egusphere-2025-2559
Preprint. Discussion started: 1 July 2025

References

Aas, W.: Measurement of Temperature at Zeppelin Mountain (Ny-Ålesund), https://doi.org/10.48597/RP9S-9PKU, 2015.

Aas, W.: Measurement of Temperature at Zeppelin Mountain (Ny-Ålesund), https://doi.org/10.48597/2MF2-3X96, 2016.

Aas, W.: Measurement of Meteorology at Zeppelin Mountain (Ny-Ålesund), https://doi.org/10.48597/V3MN-G5X2, 2021a.

Aas, W.: Measurement of Temperature at Zeppelin Mountain (Ny-Ålesund), https://doi.org/10.48597/84JN-CNSP, 2021b.

Aas, W.: Measurement of Meteorology at Zeppelin Mountain (Ny-Ålesund), https://doi.org/10.48597/3N4J-7DMB, 2022.

Abdul-Razzak, H. and Ghan, S. J.: A Parameterization of Aerosol Activation: 2. Multiple Aerosol Types, Journal of Geophysical Research: Atmospheres, 105, 6837–6844, https://doi.org/10.1029/1999JD901161, 2000.

Abdul-Razzak, H. and Ghan, S. J.: A Parameterization of Aerosol Activation 3. Sectional Representation, Journal of Geophysical Research: Atmospheres, 107, AAC 1–1–AAC 1–6, https://doi.org/10.1029/2001JD000483, 2002.

Albrecht, B. A.: Aerosols, Cloud Microphysics, and Fractional Cloudiness, Science, 245, 1227–1230, https://doi.org/10.1126/science.245.4923.1227, 1989.

Andreae, M. O., Afchine, A., Albrecht, R., Holanda, B. A., Artaxo, P., Barbosa, H. M. J., Borrmann, S., Cecchini, M. A., Costa, A., Dollner, M., Fütterer, D., Järvinen, E., Jurkat, T., Klimach, T., Konemann, T., Knote, C., Krämer, M., Krisna, T., Machado, L. A. T., Mertes, S., Minikin, A., Pöhlker, C., Pöhlker, M. L., Pöschl, U., Rosenfeld, D., Sauer, D., Schlager, H., Schnaiter, M., Schneider, J., Schulz, C., Spanu, A., Sperling, V. B., Voigt, C., Walser, A., Wang, J., Weinzierl, B., Wendisch, M., and Ziereis, H.: Aerosol Characteristics and Particle Production in the Upper Troposphere over the Amazon Basin, Atmospheric Chemistry and Physics, 18, 921–961, https://doi.org/10.5194/acp-18-921-2018, 2018.

Balkanski, Y. J., Jacob, D. J., Gardner, G. M., Graustein, W. C., and Turekian, K. K.: Transport and Residence Times of Tropospheric Aerosols Inferred from a Global Three-Dimensional Simulation of 210Pb, Journal of Geophysical Research: Atmospheres, 98, 20 573–20 586, https://doi.org/10.1029/93JD02456, 1993.

Bardakov, R., Thornton, J. A., Ekman, A. M. L., Krejci, R., Pöhlker, M. L., Curtius, J., Williams, J., Lelieveld, J., and Riipinen, I.: High Concentrations of Nanoparticles From Isoprene Nitrates Predicted in Convective Outflow Over the Amazon, Geophysical Research Letters, 51, e2024GL109 919, https://doi.org/10.1029/2024GL109919, 2024.

Barth, M. C., Rasch, P. J., Kiehl, J. T., Benkovitz, C. M., and Schwartz, S. E.: Sulfur Chemistry in the National Center for Atmospheric Research Community Climate Model: Description, Evaluation, Features, and Sensitivity to Aqueous Chemistry, Journal of Geophysical Research: Atmospheres, 105, 1387–1415, https://doi.org/10.1029/1999JD900773, 2000.

Bechtold, P., Semane, N., Lopez, P., Chaboureau, J.-P., Beljaars, A., and Bormann, N.: Representing Equilibrium and Nonequilibrium Convection in Large-Scale Models, https://doi.org/10.1175/JAS-D-13-0163.1, 2014.

Bentsen, M., Bethke, I., Debernard, J. B., Iversen, T., Kirkevåg, A., Seland, Ø., Drange, H., Roelandt, C., Seierstad, I. A., Hoose, C., and Kristjánsson, J. E.: The Norwegian Earth System Model, NorESM1-M – Part 1: Description and Basic Evaluation of the Physical Climate, Geoscientific Model Development, 6, 687–720, https://doi.org/10.5194/gmd-6-687-2013, 2013.

Bergeron, T.: On the Physics of Cloud and Precipitation: Mémoire Présenté a L'association de Météorologie de L'UGGI, Lisbonne, September 1933, Imprimerie Paul Dupont, 1935.

Bergman, T., Kerminen, V.-M., Korhonen, H., Lehtinen, K. J., Makkonen, R., Arola, A., Mielonen, T., Romakkaniemi, S., Kulmala, M., and Kokkola, H.: Evaluation of the Sectional Aerosol Microphysics Module SALSA Implementation in ECHAM5-HAM Aerosol-Climate Model, Geoscientific Model Development, 5, 845–868, https://doi.org/10.5194/gmd-5-845-2012, 2012.

https://doi.org/10.5194/egusphere-2025-2559
Preprint. Discussion started: 1 July 2025

Berrisford, P., Dee, D. P., Poli, P., Brugge, R., Fielding, M., Fuentes, M., Kållberg, P. W., Kobayashi, S., Uppala, S., and Simmons, A.: The ERA-Interim Archive Version 2.0, 2011.

Blichner, S. M.: Trajectory Precipitation and Station Data for Three GCMs and for Observations, https://doi.org/10.5281/ZENODO.15528150, 2025.

Blichner, S. M., Sporre, M. K., and Berntsen, T. K.: Reduced Effective Radiative Forcing from Cloud–Aerosol Interactions (ERFaci) with Improved Treatment of Early Aerosol Growth in an Earth System Model, Atmospheric Chemistry and Physics, 21, 17 243–17 265, https://doi.org/10.5194/acp-21-17243-2021, 2021.

Blichner, S. M., Yli-Juuti, T., Mielonen, T., Pöhlker, C., Holopainen, E., Heikkinen, L., Mohr, C., Artaxo, P., Carbone, S., Meller, B. B., Quaresma Dias-Júnior, C., Kulmala, M., Petäjä, T., Scott, C. E., Svenhag, C., Nieradzik, L., Sporre, M., Partridge, D. G., Tovazzi, E., Virtanen, A., Kokkola, H., and Riipinen, I.: Process-Evaluation of Forest Aerosol-Cloud-Climate Feedback Shows Clear Evidence from Observations and Large Uncertainty in Models, Nature Communications, 15, 969, https://doi.org/10.1038/s41467-024-45001-y, 2024.

Bogenschutz, P. A., Gettelman, A., Hannay, C., Larson, V. E., Neale, R. B., Craig, C., and Chen, C.-C.: The Path to CAM6: Coupled Simulations with CAM5.4 and CAM5.5, Geoscientific Model Development, 11, 235–255, https://doi.org/10.5194/gmd-11-235-2018, 2018.

Bourgeois, Q. and Bey, I.: Pollution Transport Efficiency toward the Arctic: Sensitivity to Aerosol Scavenging and Source Regions, Journal of Geophysical Research: Atmospheres, 116, https://doi.org/10.1029/2010JD015096, 2011.

Browse, J., Carslaw, K. S., Arnold, S. R., Pringle, K., and Boucher, O.: The Scavenging Processes Controlling the Seasonal Cycle in Arctic Sulphate and Black Carbon Aerosol, Atmospheric Chemistry and Physics, 12, 6775–6798, https://doi.org/10.5194/acp-12-6775-2012, 2012.

C3S: ERA5 Hourly Data on Single Levels from 1940 to Present, https://doi.org/10.24381/CDS.ADBB2D47, 2018.

Chen, T. and Guestrin, C.: XGBoost: A Scalable Tree Boosting System, in: Proceedings of the 22nd ACM SIGKDD International Conference on Knowledge Discovery and Data Mining, Kdd '16, pp. 785–794, ACM, New York, NY, USA, ISBN 978-1-4503-4232-2, https://doi.org/10.1145/2939672.2939785, 2016.

Croft, B., Lohmann, U., Martin, R. V., Stier, P., Wurzler, S., Feichter, J., Posselt, R., and Ferrachat, S.: Aerosol Size-Dependent below-Cloud Scavenging by Rain and Snow in the ECHAM5-HAM, Atmospheric Chemistry and Physics, 9, 4653–4675, https://doi.org/10.5194/acp-9-4653-2009, 2009.

Croft, B., Lohmann, U., Martin, R. V., Stier, P., Wurzler, S., Feichter, J., Hoose, C., Heikkilä, U., van Donkelaar, A., and Ferrachat, S.: Influences of In-Cloud Aerosol Scavenging Parameterizations on Aerosol Concentrations and Wet Deposition in ECHAM5-HAM, Atmospheric Chemistry and Physics, 10, 1511–1543, https://doi.org/10.5194/acp-10-1511-2010, 2010.

Curtius, J., Heinritzi, M., Beck, L. J., Pöhlker, M. L., Tripathi, N., Krumm, B. E., Holzbeck, P., Nussbaumer, C. M., Hernández Pardo, L., Klimach, T., Barmpounis, K., Andersen, S. T., Bardakov, R., Bohn, B., Cecchini, M. A., Chaboureau, J.-P., Dauhut, T., Dienhart, D., Dörich, R., Edtbauer, A., Giez, A., Hartmann, A., Holanda, B. A., Joppe, P., Kaiser, K., Keber, T., Klebach, H., Krüger, O. O., Kürten, A., Mallaun, C., Marno, D., Martinez, M., Monteiro, C., Nelson, C., Ort, L., Raj, S. S., Richter, S., Ringsdorf, A., Rocha, F., Simon, M., Sreekumar, S., Tsokankunku, A., Unfer, G. R., Valenti, I. D., Wang, N., Zahn, A., Zauner-Wieczorek, M., Albrecht, R. I., Andreae, M. O., Artaxo, P., Crowley, J. N., Fischer, H., Harder, H., Herdies, D. L., Machado, L. A. T., Pöhlker, C., Pöschl, U., Possner, A., Pozzer, A., Schneider, J., Williams, J., and Lelieveld, J.: Isoprene Nitrates Drive New Particle Formation in Amazon's Upper Troposphere, Nature, 636, 124–130, https://doi.org/10.1038/s41586-024-08192-4, 2024.

https://doi.org/10.5194/egusphere-2025-2559
Preprint. Discussion started: 1 July 2025

Dada, L., Paasonen, P., Nieminen, T., Buenrostro Mazon, S., Kontkanen, J., Peräkylä, O., Lehtipalo, K., Hussein, T., Petäjä, T., Kerminen, V.-M., Bäck, J., and Kulmala, M.: Long-Term Analysis of Clear-Sky New Particle Formation Events and Nonevents in Hyytiälä, Atmospheric Chemistry and Physics, 17, 6227–6241, https://doi.org/10.5194/acp-17-6227-2017, 2017.

Dana, M. T. and Hales, J. M.: Statistical Aspects of the Washout of Polydisperse Aerosols, Atmospheric Environment (1967), 10, 45–50, https://doi.org/10.1016/0004-6981(76)90258-4, 1976.

Danabasoglu, G., Lamarque, J.-F., Bacmeister, J., Bailey, D. A., DuVivier, A. K., Edwards, J., Emmons, L. K., Fasullo, J., Garcia, R., Gettelman, A., Hannay, C., Holland, M. M., Large, W. G., Lauritzen, P. H., Lawrence, D. M., Lenaerts, J. T. M., Lindsay, K., Lipscomb, W. H., Mills, M. J., Neale, R., Oleson, K. W., Otto-Bliesner, B., Phillips, A. S., Sacks, W., Tilmes, S., van Kampenhout, L., Vertenstein, M., Bertini, A., Dennis, J., Deser, C., Fischer, C., Fox-Kemper, B., Kay, J. E., Kinnison, D., Kushner, P. J., Larson, V. E., Long, M. C., Mickelson, S., Moore, J. K., Nienhouse, E., Polvani, L., Rasch, P. J., and Strand, W. G.: The Community Earth System Model Version 2 (CESM2), Journal of Advances in Modeling Earth Systems, 12, e2019MS001 916, https://doi.org/10.1029/2019MS001916, 2020.

de Bruine, M., Krol, M., van Noije, T., Le Sager, P., and Röckmann, T.: The Impact of Precipitation Evaporation on the Atmospheric Aerosol Distribution in EC-Earth v3.2.0, Geoscientific Model Development, 11, 1443–1465, https://doi.org/10.5194/gmd-11-1443-2018, 2018.

Döscher, R., Acosta, M., Alessandri, A., Anthoni, P., Arsouze, T., Bergman, T., Bernardello, R., Boussetta, S., Caron, L.-P., Carver, G., Castrillo, M., Catalano, F., Cvijanovic, I., Davini, P., Dekker, E., Doblas-Reyes, F. J., Docquier, D., Echevarria, P., Fladrich, U., Fuentes-Franco, R., Gröger, M., v. Hardenberg, J., Hieronymus, J., Karami, M. P., Keskinen, J.-P., Koenigk, T., Makkonen, R., Massonnet, F., Ménégoz, M., Miller, P. A., Moreno-Chamarro, E., Nieradzik, L., van Noije, T., Nolan, P., O'Donnell, D., Ollinaho, P., van den Oord, G., Ortega, P., Prims, O. T., Ramos, A., Reerink, T., Rousset, C., Ruprich-Robert, Y., Le Sager, P., Schmith, T., Schrödner, R., Serva, F., Sicardi, V., Sloth Madsen, M., Smith, B., Tian, T., Tourigny, E., Uotila, P., Vancoppenolle, M., Wang, S., Wårlind, D., Willén, U., Wyser, K., Yang, S., Yepes-Arbós, X., and Zhang, Q.: The EC-Earth3 Earth System Model for the Coupled Model Intercomparison Project 6, Geoscientific Model Development, 15, 2973–3020, https://doi.org/10.5194/gmd-15-2973-2022, 2022.

Emerson, E. W., Katich, J. M., Schwarz, J. P., McMeeking, G. R., and Farmer, D. K.: Direct Measurements of Dry and Wet Deposition of Black Carbon Over a Grassland, Journal of Geophysical Research: Atmospheres, 123, 12,277–12,290, https://doi.org/10.1029/2018JD028954, 2018.

Ervens, B.: Modeling the Processing of Aerosol and Trace Gases in Clouds and Fogs, Chemical Reviews, 115, 4157–4198, https://doi.org/10.1021/cr5005887, 2015.

Findeisen, W.: Die Kolloidmeteorologischen Vorgänge Bei Der Niederschlagsbildung, Meteorol. Z., 55, 121–133, 1938.

Flossmann, A. I. and Wobrock, W.: A Review of Our Understanding of the Aerosol–Cloud Interaction from the Perspective of a Bin Resolved Cloud Scale Modelling, Atmospheric Research, 97, 478–497, https://doi.org/10.1016/j.atmosres.2010.05.008, 2010.

Flossmann, A. I., Hall, W. D., and Pruppacher, H. R.: A Theoretical Study of the Wet Removal of Atmospheric Pollutants. Part I: The Redistribution of Aerosol Particles Captured through Nucleation and Impaction Scavenging by Growing Cloud Drops, 1985.

Forster, P., Storelvmo, T., Armour, K., Collins, W., Dufresne, J.-L., Frame, D., Lunt, D. J., Mauritsen, T., Palmer, M. D., Watanabe, M., Wild, M., and Zhang, X.: The Earth's Energy Budget, Climate Feedbacks, and Climate Sensitivity, in: Climate Change 2021: The Physical Science Basis. Contribution of Working Group I to the Sixth Assessment Report of the Intergovernmental Panel on Climate Change, edited by Masson-Delmotte, V., Zhai, P., Pirani, A., Connors, S. L., Péan, C., Berger, S., Caud, N., Chen, Y., Goldfarb, L., Gomis, M. I., Huang, M., Leitzell, K., Lonnoy, E., Matthews, J. B. R., Maycock, T. K., Waterfield, T., Yelekçi, Ö., Yu, R., and Zhou, B., Cambridge University Press, 2021.

https://doi.org/10.5194/egusphere-2025-2559
Preprint. Discussion started: 1 July 2025

Franco, M. A., Ditas, F., Kremper, L. A., Machado, L. A. T., Andreae, M. O., Araújo, A., Barbosa, H. M. J., de Brito, J. F., Carbone, S., Holanda, B. A., Morais, F. G., Nascimento, J. P., Pöhlker, M. L., Rizzo, L. V., Sá, M., Saturno, J., Walter, D., Wolff, S., Pöschl, U., Artaxo, P., and Pöhlker, C.: Occurrence and Growth of Sub-50 Nm Aerosol Particles in the Amazonian Boundary Layer, Atmospheric Chemistry and Physics, 22, 3469–3492, https://doi.org/10.5194/acp-22-3469-2022, 2022.

Gettelman, A. and Morrison, H.: Advanced Two-Moment Bulk Microphysics for Global Models. Part I: Off-Line Tests and Comparison with Other Schemes, Journal of Climate, 28, 1268–1287, https://doi.org/10.1175/JCLI-D-14-00102.1, 2015.

Gordon, H., Kirkby, J., Baltensperger, U., Bianchi, F., Breitenlechner, M., Curtius, J., Dias, A., Dommen, J., Donahue, N. M., Dunne, E. M., Duplissy, J., Ehrhart, S., Flagan, R. C., Frege, C., Fuchs, C., Hansel, A., Hoyle, C. R., Kulmala, M., Kürten, A., Lehtipalo, K., Makhmutov, V., Molteni, U., Rissanen, M. P., Stozkhov, Y., Tröstl, J., Tsagkogeorgas, G., Wagner, R., Williamson, C., Wimmer, D., Winkler, P. M., Yan, C., and Carslaw, K. S.: Causes and Importance of New Particle Formation in the Present-Day and Preindustrial Atmospheres: CAUSES AND ROLE OF NEW PARTICLE FORMATION, Journal of Geophysical Research: Atmospheres, 122, 8739–8760, https://doi.org/10.1002/2017JD026844, 2017.

Greenfield, S. M.: RAIN SCAVENGING OF RADIOACTIVE PARTICULATE MATTER FROM THE ATMOSPHERE, 1957.

Hakala, S., Alghamdi, M. A., Paasonen, P., Vakkari, V., Khoder, M. I., Neitola, K., Dada, L., Abdelmaksoud, A. S., Al-Jeelani, H., Shabbaj, I. I., Almehmadi, F. M., Sundström, A.-M., Lihavainen, H., Kerminen, V.-M., Kontkanen, J., Kulmala, M., Hussein, T., and Hyvärinen, A.-P.: New Particle Formation, Growth and Apparent Shrinkage at a Rural Background Site in Western Saudi Arabia, Atmospheric Chemistry and Physics, 19, 10 537–10 555, https://doi.org/10.5194/acp-19-10537-2019, 2019.

Heikkinen, L., Äijälä, M., Riva, M., Luoma, K., Dällenbach, K., Aalto, J., Aalto, P., Aliaga, D., Aurela, M., Keskinen, H., Makkonen, U., Rantala, P., Kulmala, M., Petäjä, T., Worsnop, D., and Ehn, M.: Long-Term Sub-Micrometer Aerosol Chemical Composition in the Boreal Forest: Inter- and Intra-Annual Variability, Atmospheric Chemistry and Physics, 20, 3151–3180, https://doi.org/10.5194/acp-20-3151-2020, 2020.

Heslin-Rees, D., Tunved, P., Ström, J., Cremer, R., Zieger, P., Riipinen, I., Ekman, A. M. L., Eleftheriadis, K., and Krejci, R.: Increase in Precipitation Scavenging Contributes to Long-Term Reductions of Light-Absorbing Aerosol in the Arctic, Atmospheric Chemistry and Physics, 24, 2059–2075, https://doi.org/10.5194/acp-24-2059-2024, 2024.

Holopainen, E., Kokkola, H., Laakso, A., and Kühn, T.: In-Cloud Scavenging Scheme for Sectional Aerosol Modules – Implementation in the Framework of the Sectional Aerosol Module for Large Scale Applications Version 2.0 (SALSA2.0) Global Aerosol Module, Geoscientific Model Development, 13, 6215–6235, https://doi.org/10.5194/gmd-13-6215-2020, 2020.

Hoose, C., Lohmann, U., Bennartz, R., Croft, B., and Lesins, G.: Global Simulations of Aerosol Processing in Clouds, Atmospheric Chemistry and Physics, 8, 6939–6963, https://doi.org/10.5194/acp-8-6939-2008, 2008a.

Hoose, C., Lohmann, U., Stier, P., Verheggen, B., and Weingartner, E.: Aerosol Processing in Mixed-Phase Clouds in ECHAM5-HAM: Model Description and Comparison to Observations, Journal of Geophysical Research: Atmospheres, 113, https://doi.org/10.1029/2007JD009251, 2008b.

Hurrell, J. W., Hack, J. J., Shea, D., Caron, J. M., and Rosinski, J.: A New Sea Surface Temperature and Sea Ice Boundary Dataset for the Community Atmosphere Model, Journal of Climate, 21, 5145–5153, https://doi.org/10.1175/2008JCLI2292.1, 2008.

Irfan, M., Kühn, T., Yli-Juuti, T., Laakso, A., Holopainen, E., Worsnop, D. R., Virtanen, A., and Kokkola, H.: A Model Study Investigating the Sensitivity of Aerosol Forcing to the Volatilities of Semi-Volatile Organic Compounds, Atmospheric Chemistry and Physics, 24, 8489–8506, https://doi.org/10.5194/acp-24-8489-2024, 2024.

https://doi.org/10.5194/egusphere-2025-2559
Preprint. Discussion started: 1 July 2025

Isokääntä, S., Kim, P., Mikkonen, S., Kühn, T., Kokkola, H., Yli-Juuti, T., Heikkinen, L., Luoma, K., Petäjä, T., Kipling, Z., Partridge, D., and Virtanen, A.: The Effect of Clouds and Precipitation on the Aerosol Concentrations and Composition in a Boreal Forest Environment, Atmospheric Chemistry and Physics, 22, 11 823–11 843, https://doi.org/10.5194/acp-22-11823-2022, 2022.

Iversen, T. and Seland, Ø.: A Scheme for Process-Tagged SO4 and BC Aerosols in NCAR CCM3: Validation and Sensitivity to Cloud Processes, Journal of Geophysical Research: Atmospheres, 107, 4751, https://doi.org/10.1029/2001JD000885, 2002.

Iversen, T., Bentsen, M., Bethke, I., Debernard, J. B., Kirkevåg, A., Seland, Ø., Drange, H., Kristjansson, J. E., Medhaug, I., Sand, M., and Seierstad, I. A.: The Norwegian Earth System Model, NorESM1-M – Part 2: Climate Response and Scenario Projections, Geoscientific Model Development, 6, 389–415, https://doi.org/10.5194/gmd-6-389-2013, 2013.

Jokinen, T., Kontkanen, J., Lehtipalo, K., Manninen, H. E., Aalto, J., Porcar-Castell, A., Garmash, O., Nieminen, T., Ehn, M., Kangasluoma, J., Junninen, H., Levula, J., Duplissy, J., Ahonen, L. R., Rantala, P., Heikkinen, L., Yan, C., Sipilä, M., Worsnop, D. R., Bäck, J., Petäjä, T., Kerminen, V.-M., and Kulmala, M.: Solar Eclipse Demonstrating the Importance of Photochemistry in New Particle Formation, Scientific Reports, 7, 45 707, https://doi.org/10.1038/srep45707, 2017.

Khadir, T.: PNSDs and Trajectory History Datasets (Khadir et al., 2023), https://doi.org/10.5281/ZENODO.7907473, 2023.

Khadir, T., Riipinen, I., Talvinen, S., Heslin-Rees, D., Pöhlker, C., Rizzo, L., Machado, L. A. T., Franco, M. A., Kremper, L. A., Artaxo, P., Petäjä, T., Kulmala, M., Tunved, P., Ekman, A. M. L., Krejci, R., and Virtanen, A.: Sink, Source or Something In-Between? Net Effects of Precipitation on Aerosol Particle Populations, Geophysical Research Letters, 50, e2023GL104 325, https://doi.org/10.1029/2023GL104325, 2023.

Kipling, Z., Stier, P., Johnson, C. E., Mann, G. W., Bellouin, N., Bauer, S. E., Bergman, T., Chin, M., Diehl, T., Ghan, S. J., Iversen, T., Kirkevåg, A., Kokkola, H., Liu, X., Luo, G., van Noije, T., Pringle, K. J., von Salzen, K., Schulz, M., Seland, Ø., Skeie, R. B., Takemura, T., Tsigaridis, K., and Zhang, K.: What Controls the Vertical Distribution of Aerosol? Relationships between Process Sensitivity in HadGEM3–UKCA and Inter-Model Variation from AeroCom Phase II, Atmospheric Chemistry and Physics, 16, 2221–2241, https://doi.org/10.5194/acp-16-2221-2016, 2016.

Kirkevåg, A., Iversen, T., Seland, Ø., Hoose, C., Kristjánsson, J. E., Struthers, H., Ekman, A. M. L., Ghan, S., Griesfeller, J., Nilsson, E. D., and Schulz, M.: Aerosol–Climate Interactions in the Norwegian Earth System Model – NorESM1-M, Geosci. Model Dev., 6, 207–244, https://doi.org/10.5194/gmd-6-207-2013, 2013.

Kirkevåg, A., Grini, A., Olivié, D., Seland, Ø., Alterskjær, K., Hummel, M., Karset, I. H. H., Lewinschal, A., Liu, X., Makkonen, R., Bethke, I., Griesfeller, J., Schulz, M., and Iversen, T.: A Production-Tagged Aerosol Module for Earth System Models, OsloAero5.3 – Extensions and Updates for CAM5.3-Oslo, Geoscientific Model Development, 11, 3945–3982, https://doi.org/10.5194/gmd-11-3945-2018, 2018.

Kokkola, H., Kühn, T., Laakso, A., Bergman, T., Lehtinen, K. E. J., Mielonen, T., Arola, A., Stadtler, S., Korhonen, H., Ferrachat, S., Lohmann, U., Neubauer, D., Tegen, I., Siegenthaler-Le Drian, C., Schultz, M. G., Bey, I., Stier, P., Daskalakis, N., Heald, C. L., and Romakkaniemi, S.: SALSA2.0: The Sectional Aerosol Module of the Aerosol–Chemistry–Climate Model ECHAM6.3.0-HAM2.3-MOZ1.0, Geoscientific Model Development, 11, 3833–3863, https://doi.org/10.5194/gmd-11-3833-2018, 2018.

Krol, M., Houweling, S., Bregman, B., van den Broek, M., Segers, A., van Velthoven, P., Peters, W., Dentener, F., and Bergamaschi, P.: The Two-Way Nested Global Chemistry-Transport Zoom Model TM5: Algorithm and Applications, Atmospheric Chemistry and Physics, 5, 417–432, https://doi.org/10.5194/acp-5-417-2005, 2005.

Kulmala, M. and Petäjä, T.: Measurement of Meteorology at Hyytiälä, https://doi.org/10.48597/N5C6-V7QN, 2024.

https://doi.org/10.5194/egusphere-2025-2559
Preprint. Discussion started: 1 July 2025

Kulmala, M., Vehkamäki, H., Petäjä, T., Dal Maso, M., Lauri, A., Kerminen, V.-M., Birmili, W., and McMurry, P.: Formation and Growth Rates of Ultrafine Atmospheric Particles: A Review of Observations, Journal of Aerosol Science, 35, 143–176, https://doi.org/10.1016/j.jaerosci.2003.10.003, 2004.

Lee, H., Lee, K., Lunder, C. R., Krejci, R., Aas, W., Park, J., Park, K.-T., Lee, B. Y., Yoon, Y. J., and Park, K.: Atmospheric New Particle Formation Characteristics in the Arctic as Measured at Mount Zeppelin, Svalbard, from 2016 to 2018, Atmospheric Chemistry and Physics, 20, 13 425–13 441, https://doi.org/10.5194/acp-20-13425-2020, 2020.

Lelieveld, J., Klingmüller, K., Pozzer, A., Burnett, R. T., Haines, A., and Ramanathan, V.: Effects of Fossil Fuel and Total Anthropogenic Emission Removal on Public Health and Climate, Proceedings of the National Academy of Sciences, 116, 7192–7197, https://doi.org/10.1073/pnas.1819989116, 2019.

Lohmann, U., Leaitch, W. R., Barrie, L., Law, K., Yi, Y., Bergmann, D., Bridgeman, C., Chin, M., Christensen, J., Easter, R., Feichter, J., Jeuken, A., Kjellström, E., Koch, D., Land, C., Rasch, P., and Roelofs, G.-J.: Vertical Distributions of Sulfur Species Simulated by Large Scale Atmospheric Models in COSAM: Comparison with Observations, Tellus B, 53, 646–672, https://doi.org/10.1034/j.1600-0889.2001.530508.x, 2001.

Lundberg, S. and Lee, S.-I.: A Unified Approach to Interpreting Model Predictions, https://doi.org/10.48550/arXiv.1705.07874, 2017.

Luoma, K., Virkkula, A., Aalto, P., Petäjä, T., and Kulmala, M.: Over a 10-Year Record of Aerosol Optical Properties at SMEAR II, Atmospheric Chemistry and Physics, 19, 11 363–11 382, https://doi.org/10.5194/acp-19-11363-2019, 2019.

Machado, L. A. T., Unfer, G. R., Brill, S., Hildmann, S., Pöhlker, C., Cheng, Y., Williams, J., Hartwig, H., Andreae, M. O., Artaxo, P., Curtius, J., Franco, M. A., Cecchini, M. A., Edtbauer, A., Hoffmann, T., Holanda, B., Khadir, T., Krejci, R., Kremper, L. A., Liu, Y., Meller, B. B., Pöhlker, M. L., Quesada, C. A., Ringsdorf, A., Riipinen, I., Trumbore, S., Wolff, S., Lelieveld, J., and Pöschl, U.: Frequent Rainfall-Induced New Particle Formation within the Canopy in the Amazon Rainforest, Nature Geoscience, 17, 1225–1232, https://doi.org/10.1038/s41561-024-01585-0, 2024.

Marshall, J. S. and Palmer, W. M. K.: THE DISTRIBUTION OF RAINDROPS WITH SIZE, 1948.

Merikanto, J., Spracklen, D. V., Mann, G. W., Pickering, S. J., and Carslaw, K. S.: Impact of Nucleation on Global CCN, Atmos. Chem. Phys., 9, 8601–8616, https://doi.org/10.5194/acp-9-8601-2009, 2009.

Michot, V., Vila, D., Arvor, D., Corpetti, T., Ronchail, J., Funatsu, B. M., and Dubreuil, V.: Performance of TRMM TMPA 3B42 V7 in Replicating Daily Rainfall and Regional Rainfall Regimes in the Amazon Basin (1998–2013), Remote Sensing, 10, 1879, https://doi.org/10.3390/rs10121879, 2018.

Mielonen, T., Hienola, A., Kühn, T., Merikanto, J., Lipponen, A., Bergman, T., Korhonen, H., Kolmonen, P., Sogacheva, L., Ghent, D., Pitkänen, M. R. A., Arola, A., De Leeuw, G., and Kokkola, H.: Summertime Aerosol Radiative Effects and Their Dependence on Temperature over the Southeastern USA, Atmosphere, 9, 180, https://doi.org/10.3390/atmos9050180, 2018.

Moseid, K. O., Schulz, M., Storelvmo, T., Julsrud, I. R., Olivié, D., Nabat, P., Wild, M., Cole, J. N. S., Takemura, T., Oshima, N., Bauer, S. E., and Gastineau, G.: Bias in CMIP6 Models as Compared to Observed Regional Dimming and Brightening, Atmospheric Chemistry and Physics, 20, 16 023–16 040, https://doi.org/10.5194/acp-20-16023-2020, 2020.

Moteki, N., Kondo, Y., Oshima, N., Takegawa, N., Koike, M., Kita, K., Matsui, H., and Kajino, M.: Size Dependence of Wet Removal of Black Carbon Aerosols during Transport from the Boundary Layer to the Free Troposphere, Geophysical Research Letters, 39, https://doi.org/10.1029/2012GL052034, 2012.

https://doi.org/10.5194/egusphere-2025-2559
Preprint. Discussion started: 1 July 2025

Nordeng, T.-E.: Extended Versions of the Convective Parametrization Scheme at ECMWF and Their Impact on the Mean and Transient Activity of the Model in the Tropics, https://www.ecmwf.int/en/elibrary/75843-extended-versions-convective-parametrization-scheme-ecmwf-and-their-impact-mean, 1994.

Ohata, S., Moteki, N., Mori, T., Koike, M., and Kondo, Y.: A Key Process Controlling the Wet Removal of Aerosols: New Observational Evidence, Scientific Reports, 6, 34 113, https://doi.org/10.1038/srep34113, 2016.

Olenius, T. and Riipinen, I.: Molecular-Resolution Simulations of New Particle Formation: Evaluation of Common Assumptions Made in Describing Nucleation in Aerosol Dynamics Models, Aerosol Science and Technology, 51, 397–408, https://doi.org/10.1080/02786826.2016.1262530, 2017.

Patoulias, D., Florou, K., Pandis, S. N., and Nenes, A.: New Particle Formation Events Can Reduce Cloud Droplets in Boundary Layer Clouds at the Continental Scale, Geophysical Research Letters, 51, e2023GL106 182, https://doi.org/10.1029/2023GL106182, 2024.

Pruppacher, H. R., Klett, J. D., and Wang, P. K.: Microphysics of Clouds and Precipitation, Aerosol Science and Technology, 28, 381–382, https://doi.org/10.1080/02786829808965531, 1998.

Ranjan, R., Heikkinen, L., Ahonen, L. R., Luoma, K., Bowen, P., Petäjä, T., Ekman, A. M. L., Partridge, D. G., and Riipinen, I.: Optimizing CCN Predictions through Inferred Modal Aerosol Composition – a Boreal Forest Case Study, EGUsphere, pp. 1–35, https://doi.org/10.5194/egusphere-2025-1602, 2025.

Rayner, N. A., Parker, D. E., Horton, E. B., Folland, C. K., Alexander, L. V., Rowell, D. P., Kent, E. C., and Kaplan, A.: Global Analyses of Sea Surface Temperature, Sea Ice, and Night Marine Air Temperature since the Late Nineteenth Century, Journal of Geophysical Research: Atmospheres, 108, https://doi.org/10.1029/2002JD002670, 2003.

Roldin, P., Ehn, M., Kurtén, T., Olenius, T., Rissanen, M. P., Sarnela, N., Elm, J., Rantala, P., Hao, L., Hyttinen, N., Heikkinen, L., Worsnop, D. R., Pichelstorfer, L., Xavier, C., Clusius, P., Öström, E., Petäjä, T., Kulmala, M., Vehkamäki, H., Virtanen, A., Riipinen, I., and Boy, M.: The Role of Highly Oxygenated Organic Molecules in the Boreal Aerosol-Cloud-Climate System, Nature Communications, 10, 4370, https://doi.org/10.1038/s41467-019-12338-8, 2019.

Ryu, Y.-H. and Min, S.-K.: Improving Wet and Dry Deposition of Aerosols in WRF-Chem: Updates to Below-Cloud Scavenging and Coarse-Particle Dry Deposition, Journal of Advances in Modeling Earth Systems, 14, e2021MS002 792, https://doi.org/10.1029/2021MS002792, 2022.

Schraufnagel, D. E.: The Health Effects of Ultrafine Particles, Experimental & Molecular Medicine, 52, 311–317, https://doi.org/10.1038/s12276-020-0403-3, 2020.

Schultz, M. G., Stadtler, S., Schröder, S., Taraborrelli, D., Franco, B., Krefting, J., Henrot, A., Ferrachat, S., Lohmann, U., Neubauer, D., Siegenthaler-Le Drian, C., Wahl, S., Kokkola, H., Kühn, T., Rast, S., Schmidt, H., Stier, P., Kinnison, D., Tyndall, G. S., Orlando, J. J., and Wespes, C.: The Chemistry–Climate Model ECHAM6.3-HAM2.3-MOZ1.0, Geosci. Model Dev., 11, 1695–1723, https://doi.org/10.5194/gmd-11-1695-2018, 2018.

Seinfeld, J. H. and Pandis, S. N.: Atmospheric Chemistry and Physics, John Wiley & Sons, New Jersey, 3 edn., 2016.

Seland, ø., Iversen, T., KirkevåG, A., and Storelvmo, T.: Aerosol-Climate Interactions in the CAM-Oslo Atmospheric GCM and Investigation of Associated Basic Shortcomings, Tellus A, 60, 459–491, https://doi.org/10.1111/j.1600-0870.2008.00318.x, 2008.

Seland, Ø., Bentsen, M., Olivié, D., Toniazzo, T., Gjermundsen, A., Graff, L. S., Debernard, J. B., Gupta, A. K., He, Y.-C., Kirkevåg, A., Schwinger, J., Tjiputra, J., Aas, K. S., Bethke, I., Fan, Y., Griesfeller, J., Grini, A., Guo, C., Ilicak, M., Karset, I. H. H., Landgren, O., Liakka, J., Moseid, K. O., Nummelin, A., Spensberger, C., Tang, H., Zhang, Z., Heinze, C., Iversen, T., and Schulz, M.: Overview of

https://doi.org/10.5194/egusphere-2025-2559
Preprint. Discussion started: 1 July 2025

the Norwegian Earth System Model (NorESM2) and Key Climate Response of CMIP6 DECK, Historical, and Scenario Simulations, Geoscientific Model Development, 13, 6165–6200, https://doi.org/10.5194/gmd-13-6165-2020, 2020.

Shapley, L. S.: 17. A Value for n-Person Games, in: Contributions to the Theory of Games (AM-28), Volume II, pp. 307–318, Princeton University Press, ISBN 978-1-4008-8197-0, https://doi.org/10.1515/9781400881970-018, 1953.

Shen, J., Russell, D. M., DeVivo, J., Kunkler, F., Baalbaki, R., Mentler, B., Scholz, W., Yu, W., Caudillo-Plath, L., Sommer, E., Ahongshangbam, E., Alfaouri, D., Almeida, J., Amorim, A., Beck, L. J., Beckmann, H., Berntheusel, M., Bhattacharyya, N., Canagaratna, M. R., Chassaing, A., Cruz-Simbron, R., Dada, L., Duplissy, J., Gordon, H., Granzin, M., Große Schute, L., Heinritzi, M., Iyer, S., Klebach, H., Krüger, T., Kürten, A., Lampimäki, M., Liu, L., Lopez, B., Martinez, M., Morawiec, A., Onnela, A., Peltola, M., Rato, P., Reza, M., Richter, S., Rörup, B., Sebastian, M. K., Simon, M., Surdu, M., Tamme, K., Thakur, R. C., Tomé, A., Tong, Y., Top, J., Umo, N. S., Unfer, G., Vettikkat, L., Weissbacher, J., Xenofontos, C., Yang, B., Zauner-Wieczorek, M., Zhang, J., Zheng, Z., Baltensperger, U., Christoudias, T., Flagan, R. C., El Haddad, I., Junninen, H., Möhler, O., Riipinen, I., Rohner, U., Schobesberger, S., Volkamer, R., Winkler, P. M., Hansel, A., Lehtipalo, K., Donahue, N. M., Lelieveld, J., Harder, H., Kulmala, M., Worsnop, D. R., Kirkby, J., Curtius, J., and He, X.-C.: New Particle Formation from Isoprene under Upper-Tropospheric Conditions, Nature, 636, 115–123, https://doi.org/10.1038/s41586-024-08196-0, 2024.

Slinn, W. G. N.: Precipitation Scavenging, in: Atmospheric Science and Power Production, edited by Randerson, D., chap. 11, pp. 466–532, Technical Information Center, Office of Scientific and Technical Information, U.S. Department of Energy, Washington, DC, USA, 1984.

Stier, P., Feichter, J., Kinne, S., Kloster, S., Vignati, E., Wilson, J., Ganzeveld, L., Tegen, I., Werner, M., Balkanski, Y., Schulz, M., Boucher, O., Minikin, A., and Petzold, A.: The Aerosol-Climate Model ECHAM5-HAM, Atmospheric Chemistry and Physics, 5, 1125–1156, https://doi.org/10.5194/acp-5-1125-2005, 2005.

Stolzenburg, D., Cai, R., Blichner, S. M., Kontkanen, J., Zhou, P., Makkonen, R., Kerminen, V.-M., Kulmala, M., Riipinen, I., and Kangasluoma, J.: Atmospheric Nanoparticle Growth, Reviews of Modern Physics, 95, 045 002, https://doi.org/10.1103/RevModPhys.95.045002, 2023.

Sullivan, R. C., Crippa, P., Matsui, H., Leung, L. R., Zhao, C., Thota, A., and Pryor, S. C.: New Particle Formation Leads to Cloud Dimming, npj Climate and Atmospheric Science, 1, 1–9, https://doi.org/10.1038/s41612-018-0019-7, 2018.

Svenhag, C., Sporre, M. K., Olenius, T., Yazgi, D., Blichner, S. M., Nieradzik, L. P., and Roldin, P.: Implementing Detailed Nucleation Predictions in the Earth System Model EC-Earth3.3.4: Sulfuric Acid–Ammonia Nucleation, Geoscientific Model Development, 17, 4923–4942, https://doi.org/10.5194/gmd-17-4923-2024, 2024.

Talvinen, S., Kim, P., Tovazzi, E., Holopainen, E., Cremer, R., Kühn, T., Kokkola, H., Kipling, Z., Neubauer, D., Teixeira, J. C., Sellar, A., Watson-Parris, D., Yang, Y., Zhu, J., Krishnan, S., Virtanen, A., and Partridge, D. G.: Towards an Improved Understanding of the Impact of Clouds and Precipitation on the Representation of Aerosols over the Boreal Forest in GCMs, EGUsphere, pp. 1–49, https://doi.org/10.5194/egusphere-2025-721, 2025.

Taylor, J. W., Allan, J. D., Allen, G., Coe, H., Williams, P. I., Flynn, M. J., Le Breton, M., Muller, J. B. A., Percival, C. J., Oram, D., Forster, G., Lee, J. D., Rickard, A. R., Parrington, M., and Palmer, P. I.: Size-Dependent Wet Removal of Black Carbon in Canadian Biomass Burning Plumes, Atmospheric Chemistry and Physics, 14, 13 755–13 771, https://doi.org/10.5194/acp-14-13755-2014, 2014.

Tegen, I., Neubauer, D., Ferrachat, S., Siegenthaler-Le Drian, C., Bey, I., Schutgens, N., Stier, P., Watson-Parris, D., Stanelle, T., Schmidt, H., Rast, S., Kokkola, H., Schultz, M., Schroeder, S., Daskalakis, N., Barthel, S., Heinold, B., and Lohmann, U.: The Global Aerosol–Climate Model ECHAM6.3–HAM2.3 – Part 1: Aerosol Evaluation, Geoscientific Model Development, 12, 1643–1677, https://doi.org/10.5194/gmd-12-1643-2019, 2019.

https://doi.org/10.5194/egusphere-2025-2559
Preprint. Discussion started: 1 July 2025

Textor, C., Schulz, M., Guibert, S., Kinne, S., Balkanski, Y., Bauer, S., Berntsen, T., Berglen, T., Boucher, O., Chin, M., Dentener, F., Diehl, T., Easter, R., Feichter, H., Fillmore, D., Ghan, S., Ginoux, P., Gong, S., Grini, A., Hendricks, J., Horowitz, L., Huang, P., Isaksen, I., Iversen, I., Kloster, S., Koch, D., Kirkevåg, A., Kristjansson, J. E., Krol, M., Lauer, A., Lamarque, J. F., Liu, X., Montanaro, V., Myhre, G., Penner, J., Pitari, G., Reddy, S., Seland, Ø., Stier, P., Takemura, T., and Tie, X.: Analysis and Quantification of the Diversities of Aerosol Life Cycles within AeroCom, Atmospheric Chemistry and Physics, 6, 1777–1813, https://doi.org/10.5194/acp-6-1777-2006, 2006.

Tiedtke, M.: A Comprehensive Mass Flux Scheme for Cumulus Parameterization in Large-Scale Models, 1989.

Twomey, S.: The Nuclei of Natural Cloud Formation Part II: The Supersaturation in Natural Clouds and the Variation of Cloud Droplet Concentration, Geofisica pura e applicata, 43, 243–249, https://doi.org/10.1007/BF01993560, 1959.

Twomey, S.: Pollution and the Planetary Albedo, Atmospheric Environment (1967), 8, 1251–1256, https://doi.org/10.1016/0004-6981(74)90004-3, 1974.

van Noije, T., Bergman, T., Le Sager, P., O'Donnell, D., Makkonen, R., Gonçalves-Ageitos, M., Döscher, R., Fladrich, U., von Hardenberg, J., Keskinen, J.-P., Korhonen, H., Laakso, A., Myriokefalitakis, S., Ollinaho, P., Pérez García-Pando, C., Reerink, T., Schrödner, R., Wyser, K., and Yang, S.: EC-Earth3-AerChem: A Global Climate Model with Interactive Aerosols and Atmospheric Chemistry Participating in CMIP6, Geoscientific Model Development, 14, 5637–5668, https://doi.org/10.5194/gmd-14-5637-2021, 2021.

van Noije, T. P. C., Le Sager, P., Segers, A. J., van Velthoven, P. F. J., Krol, M. C., Hazeleger, W., Williams, A. G., and Chambers, S. D.: Simulation of Tropospheric Chemistry and Aerosols with the Climate Model EC-Earth, Geoscientific Model Development, 7, 2435–2475, https://doi.org/10.5194/gmd-7-2435-2014, 2014.

Vignati, E., Wilson, J., and Stier, P.: M7: An Efficient Size-Resolved Aerosol Microphysics Module for Large-Scale Aerosol Transport Models: AEROSOL MICROPHYSICS MODULE, Journal of Geophysical Research: Atmospheres, 109, n/a–n/a, https://doi.org/10.1029/2003JD004485, 2004.

Wang, J., Krejci, R., Giangrande, S., Kuang, C., Barbosa, H. M. J., Brito, J., Carbone, S., Chi, X., Comstock, J., Ditas, F., Lavric, J., Manninen, H. E., Mei, F., Moran-Zuloaga, D., Pöhlker, C., Pöhlker, M. L., Saturno, J., Schmid, B., Souza, R. A. F., Springston, S. R., Tomlinson, J. M., Toto, T., Walter, D., Wimmer, D., Smith, J. N., Kulmala, M., Machado, L. A. T., Artaxo, P., Andreae, M. O., Petäjä, T., and Martin, S. T.: Amazon Boundary Layer Aerosol Concentration Sustained by Vertical Transport during Rainfall, Nature, 539, 416–419, https://doi.org/10.1038/nature19819, 2016.

Wegener, A.: Thermodynamik Der Atmosphäre, JA Barth, 1911.

Williams, J. E., Boersma, K. F., Le Sager, P., and Verstraeten, W. W.: The High-Resolution Version of TM5-MP for Optimized Satellite Retrievals: Description and Validation, Geoscientific Model Development, 10, 721–750, https://doi.org/10.5194/gmd-10-721-2017, 2017.

Yeo, H., Kim, M.-H., Son, S.-W., Jeong, J.-H., Yoon, J.-H., Kim, B.-M., and Kim, S.-W.: Arctic Cloud Properties and Associated Radiative Effects in the Three Newer Reanalysis Datasets (ERA5, MERRA-2, JRA-55): Discrepancies and Possible Causes, Atmospheric Research, 270, 106 080, https://doi.org/10.1016/j.atmosres.2022.106080, 2022.

Zhang, G. J. and McFarlane, N. A.: Sensitivity of Climate Simulations to the Parameterization of Cumulus Convection in the Canadian Climate Centre General Circulation Model, Atmosphere-Ocean, 33, 407–446, https://doi.org/10.1080/07055900.1995.9649539, 1995.

Zhang, K., O'Donnell, D., Kazil, J., Stier, P., Kinne, S., Lohmann, U., Ferrachat, S., Croft, B., Quaas, J., Wan, H., Rast, S., and Feichter, J.: The Global Aerosol-Climate Model ECHAM-HAM, Version 2: Sensitivity to Improvements in Process Representations, Atmospheric Chemistry and Physics, 12, 8911–8949, https://doi.org/10.5194/acp-12-8911-2012, 2012.

https://doi.org/10.5194/egusphere-2025-2559
Preprint. Discussion started: 1 July 2025

Zhu, J., Li, G., Kuhn, U., Meller, B. B., Pöhlker, C., Artaxo, P., Pöschl, U., Cheng, Y., and Su, H.: Measurement Report: Number Size Distribution of Sub-40 Nm Particles in the Amazon Rainforest, EGUsphere, pp. 1–27, https://doi.org/10.5194/egusphere-2024-3911, 2025.